Archaeological and Anthropological Sciences (2025) 17:29
https://doi.org/10.1007/s12520-024-02121-2

RESEARCH

Differential metal supply networks between central and northeast Thailand, and Northwest Cambodia during the Mid-Late Iron Age: silver, copper and lead alloy artefacts from 2nd-8th c. AD Non Ban Jak

T. O. Pryce[1] · Charles Franklin Wandesforde Higham[2]

Received: 31 May 2024 / Accepted: 13 November 2024

Abstract

Sustained archaeometallurgical research since 2008 has permitted the Southeast Asian Lead Isotope Project (SEALIP) to establish the general anthropological and geochemical parameters of late prehistoric and early historic regional nonferrous base metal exchange networks. A 79 artefact assemblage from the mid-late Iron Age (2nd-8th c. AD) settlement and residential burial site of Non Ban Jak (NBJ) in lower northeast Thailand gave an opportunity to generate a fine-grained interpretation of copper-base metal supply and demand at the cusp of mainland state formation. Previous hints that the central Thai copper production centres in the Khao Wong Prachan Valley (KWPV) were only weakly active during the Iron Age, were reinforced by the near total absence of the KWPV signature at NBJ, only 165 km to the east. Since 2011, copper production at the Vilabouly Complex (VC) in central Laos has dominated regional consumption signatures, and a simple reading of the NBJ dataset would support this thesis. However, a high-density sampling shows that VC production is not actually consistent with much of NBJ consumption, and thus we must search for other Southeast Asian copper production loci. Finally, being able to analyse multiple artefacts of a range of typologies enables us to identify material culture associations between individuals at NBJ, those at other lower northeast Thai sites, and even between individuals at contemporary sites in northwest Cambodia. Intriguingly, these potential consistencies between individuals at an international scale all concern middle-aged men, possibly reinforcing regional bioarchaeological interpretations of matrilocality.

Keywords Lead isotope analysis · Provenance · Iron Age · Thailand · Southeast Asia

Highlights

Largest regional single-site archaeometallurgical study reveals 600 years of metal consumption behaviour.
Lead isotope data reveal little to no connection with central Thai copper supply but potentially west-central Thai lead/silver supply.
Non Ban Jak shares some, but not all, metal supply networks with nearby Ban Non Wat.
Multiple shared metal supply networks revealed between Mid-Late Iron Age northeast Thailand and northwest Cambodia
The hegemony of the central Lao 'Vilabouly Complex' copper supply signature begins to unravel.
First archaeometric linking of individual inhumations within and between cemeteries in Cambodia and Thailand

✉ T. O. Pryce
oliver.pryce@cnrs.fr

[1] Centre National de la Recherche Scientifique, LAPA-IRAMAT (UMR 7065) & LAPA-NIMBE (UMR 3685), CEA/CNRS, 91911 Gif-sur-Yvette, France

[2] Archaeology Programme, University of Otago, Dunedin, New Zealand

Introduction

Such is the ecological and geological diversity of Mainland Southeast Asia (MSEA), intercut with lengthy rivers and mountain ranges and interspersed with fertile plains and plateaux, it has long been acknowledged that modern national boundaries are not the ideal geographical framework within which to investigate spatio-cultural variation in the region's human past. It was upon this basis that the 'Paddy to Pura – Origins of Angkor' (P2P) project was founded in 2011, to investigate diachronic cultural interactions between northeast Thailand and northwest Cambodia. Building on previous protohistoric archaeological research in the Upper Mun River basin at Ban Lum Khao (BLK), Ban Non Wat (BNW), Noen U-Loke (NUL) and Non Muang Kao (NMK) (Higham and Thosarat 2004; Higham et al. 2007; Higham and Kijngam 2012), and in the Sisophon/Mongkol Borei River basin at Phom Sophy (PSO), Phum Snay (PSN) and Prei Khmeng (PKM) (O'Reilly et al. 2006, 2015,

Published online: 13 January 2025

2020), the P2P team carried out fresh excavations at Phum Lovea in 2011-12 and at Non Ban Jak in 2011-17 (Fig. 1). The Southeast Asian Lead Isotope Project (SEALIP), the region's first comprehensive and systematic investigation of regional copper-base production, exchange and consumption behaviours (Pryce et al. 2011a), was integrated with P2P research from the outset.

Lovea is a moated residential burial site of ca. 44 ha, located 7 km northwest of the Western Baray at Angkor (13.4841°N, 103.7130°E). An 8x8 m excavation revealed 12 burials with 14 individuals, dated AD 100–400 (O'Reilly and Shewan 2015, 2016; O'Reilly et al. 2017). The study of Lovea's material culture revealed substantial evidence for regional and inter-regional exchange, with domestic and funerary pottery analysis indicating overlapping shared ceramic traditions across NW Cambodia and NE Thailand (Lim 2020), while the technical study of 805 glass, 17 carnelian and eight agate beads suggests spheres of interaction reaching as far as the Indian subcontinent (Carter et al. 2023). In contrast, the study of Lovea's copper-base metallurgical assemblage suggested a potentially single copper source, which when, "[p]lotting the data against the known prehistoric Southeast Asian copper producers […]indicates a strong consistency with the central Lao production centre, Sepon [the Vilabouly Complex]. We use the term 'consistent' in recognition that there could be other, as yet uncharacterised, isotopic matches of primary and/or secondary production systems […]."(Pryce et al. 2017b: 398). It transpired that this interpretative caution for Iron Age interactions between Cambodia and Laos was prescient.

Site

Non Ban Jak (NBJ, 15.2586°N, 102.1703°E) is one of many Iron Age and earlier settlements that cluster on the Mun River flood plains in northeast Thailand (Fig. 2). This area was uplifted from the Shan-Thai terrane in the early Cenozoic, and its bright-red relict soils, a type of oxisol called rhodic ferralsols or Yasothon soils, overlay heavily bioturbated gravel beds (Bunopas and Vella 1992; Lofile and Kubiniok 1996). This geological history is incompatible with the formation of copper mineralisations (Hutchison and Taylor 1978; Sitthithaworn 1990), and thus any copper-base artefacts excavated at NBJ can be safely assumed to have been imported, whether as raw metal ingots or finished products.

Excavations at NBJ opened areas on two distinct mounds (Fig. 3), as well as across the moats and banks that surround the ca. 13 ha site (Higham and Kijngam 2020). NBJ was settled ca. AD 200, the subsequent mortuary sequence being

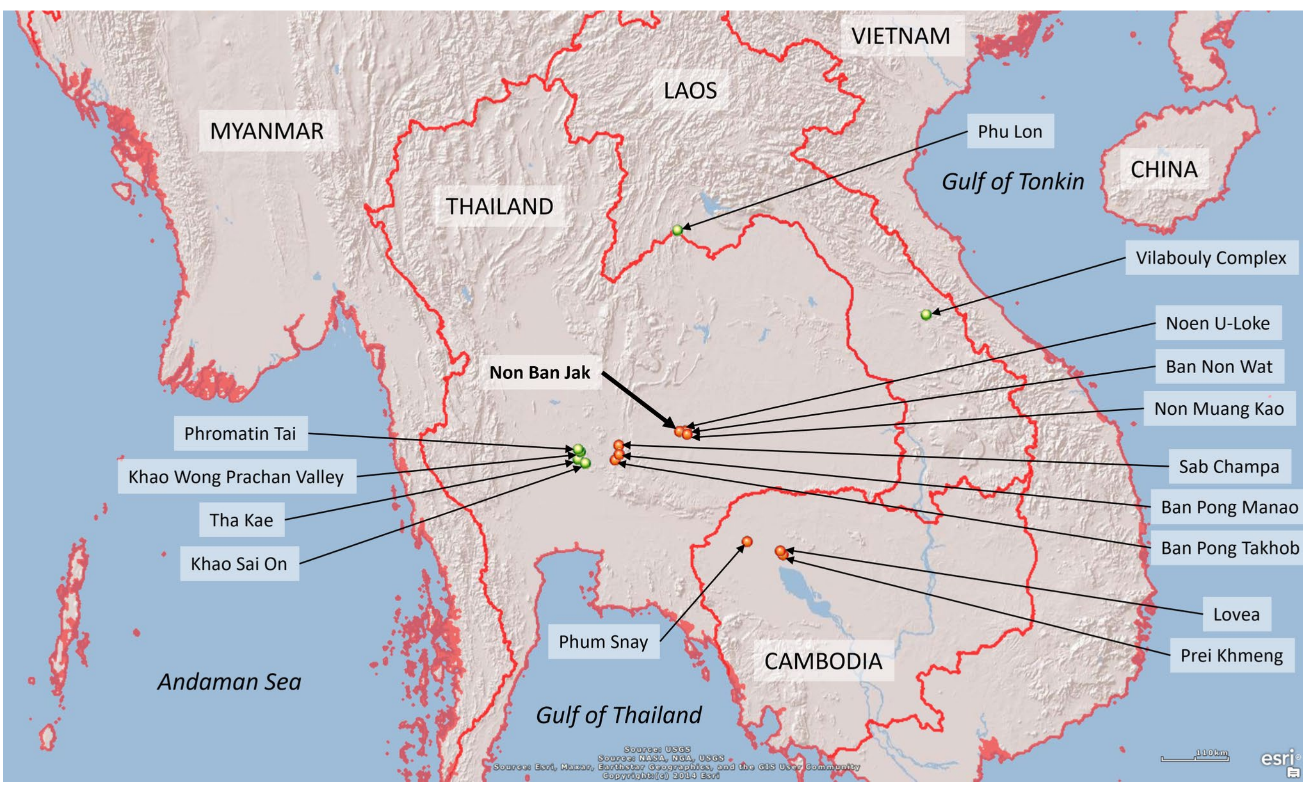

Fig. 1 Map of the region and sites mentioned in the text. Green dots represent sites with primary copper production evidence. Red dots represent copper-base consumption sites, which may also have secondary production evidence. Courtesy of ArcGIS Explorer (modified)

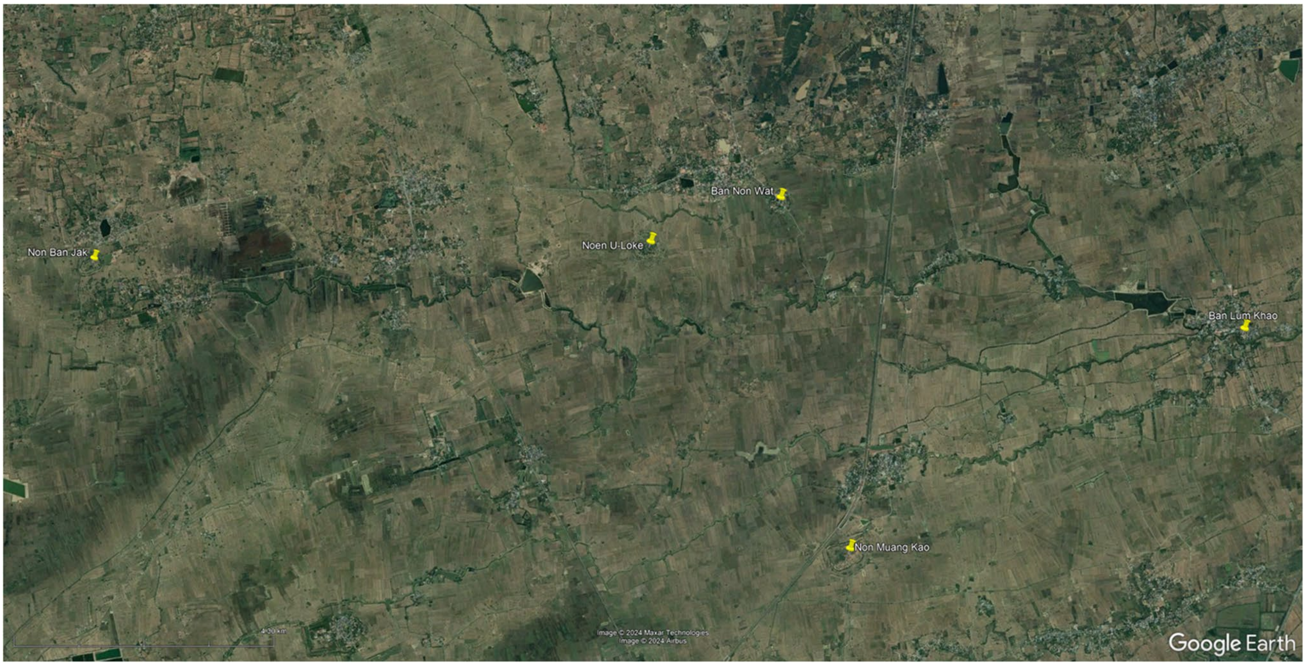

Fig. 2 Upper Mun River Valley sites excavated by the Origins of Angkor Project. Courtesy of Google Earth (modified)

divided into four phases: MP1 – AD 200–400, MP2 – AD 400–550, MP3 – AD 550–600 and MP4 – AD 600–850 (Higham et al. 2020a). This was a critical period in the later prehistory of the region, because it involved the onset of marked aridity as the strength of monsoon rains, so critical for rice cultivation, declined (Wohlfarth et al. 2016; Castillo et al. 2018). This stimulated the construction of moat/reservoirs around later Iron Age settlements, the adoption of animal-traction plough agriculture in fixed irrigated fields, and social change involving the discontinuous rise of elite leaders. This is particularly seen at the nearby site of Noen U-Loke, where, just prior to the settlement of Non Ban Jak, some men and women were interred in clusters of graves with remarkable burial wealth; incorporating gold, silver, glass, carnelian and agate ornaments, iron weapons, fine ceramic vessels, sickles and ploughshares and many copper-base ornaments (Higham et al. 2007).

At NBJ, the first settlers occupied small wattle and daub houses but, over the ensuing centuries, the growing town comprised streets flanked by stouter multi-roomed homes, with ancestors buried under the floors. Some were interred with impressive exotic ornaments, tools and weapons, including 513 copper-base artefacts with a range of typologies. Bracelets predominated, but there were also ear, finger and toe rings, belts, anklets and bells (Table 1). At no period were there as many copper-base artefacts as at Iron Age 3 Noen U-Loke, but there was a definite rise in their frequency during MP3, with a mean of 12.2 copper-base artefacts per NBJ adult burial. Despite the scale of the NBJ excavation, 664 m^2, and its focus on domestic contexts, only 60 non-mortuary copper-base artefacts and fragments thereof were found, 10.5% of the total: 14 bracelets, 11 rings, 6 'bimetallic' rings, 5 bells, 3 earrings and 25 unidentified fragments. Furthermore, although NBJ furnished substantial evidence for pottery production (Heath 2020), and limited evidence for iron smithing (Higham 2020: 38; Higham et al. 2020a: 1), only a single possible crucible fragment and no moulds or furnaces were discovered that might suggest secondary copper-base production activities - refining, alloying, founding. While a foundry could have been present on an unexcavated part of the site, based on current evidence we assume most, if not all, the copper-base artefacts were imported in finished form.

NBJ is located at a choke point for exchange, east of a pass over the Petchabun Range linking the Khorat Plateau with the plains of central Thailand (Fig. 1). The latter area is a potential source of copper (Pryce et al. 2010, 2024; Higham et al. 2020b; Cadet et al. 2024), as well as being a possible conduit to west-central Thailand, with its largely unstudied sources of lead and tin (Coote 1990; Hirao and Ro 2013; Venunan et al. 2022). It is also the likely route connecting northeast Thailand with maritime exchange networks via the Bangkok Embayment and the Gulf of Siam, which are thought to have facilitated the initial distribution of carnelian, agate and glass ornaments (Carter 2016; Bellina et al. 2019; Hoppál et al. 2023), and probably knowledge of iron smelting from South Asia from the mid-1st millennium BC (Biggs et al. 2013; Petchey et al. 2018; Venunan

Fig. 3 Aerial view of Non Ban Jak showing the areas excavated. Courtesy of Google Earth (modified)

et al. under review). Looking east from NBJ, the Mun River provides a pathway for exchange with communities up and downstream on the Mekong River, as well as beyond to the uplands of Laos and the copper mines of Vilabouly (Cadet et al. 2022). It is these metallurgical exchange network potentialities we shall investigate in the present study but it should be born in mind that in any putative exchange system, the upper Mun River region was, during the Iron Age and to this day, a major source for salt – a prerequisite for food preservation and preparation in a sub-tropical environment (Yankowski et al. 2015).

Assemblage

Focusing on the funerary assemblage, much denser in number and more securely contextualised than the domestic equivalent, of the 513 copper-base artefacts, 81 samples were taken for technological, elemental and lead isotopic analysis within the SEALIP/BROGLASEA programme (Pryce and Pigott 2024). The sampling covered the full sequence: 11 from MP1 (AD 200–400); 27 from MP2 (AD 400–550); 24 from MP3 (AD 550–600) and 17 from MP4 (AD 600–850), as well as all major typologies: 3 anklets; 28 bracelets; 2 bells; 3 belts; 10 rings; 2 earrings; 21 finger rings; two 'spirals'; 1 thumb ring; and 7 toe rings (Figures 4 and 5, Table 2). As per the nearby Ban Non Wat archaeometallurgical study (Pryce 2011), NBJ metals were heavily corroded, which will naturally impact our elemental data on a quantitative basis (Scott 2002; Selwyn 2004; Bernard and Joiret 2009) but not, we argue, on a substantive qualitative basis. Two NBJ samples, 27 and 52, were eliminated from the study in France because of near-total corrosion but nevertheless, the sampling strategy represents over 15% of the funerary copper-base artefacts. NBJ now constitutes SEALIP/BROGLASEA's most densely sampled metallurgical assemblage in Southeast Asia and will enable us to address the following research questions:

- Do the artefacts come from one or multiple sources?

Table 1 The mortuary sequence at Non Ban Jak, together with the number of copper-base artefacts found in the graves of adults and infants

MP	date AD	N burials	bracelets	finger rings	toe ring	earring	heavy ring	belts	anklet	rings in neck-lace	bell	mean/burial
Western mound burials												
MP 1 adults	100–540	7	22	1	1	0	0	0	1	0	0	4.6
MP1 infants	100–540	15	29	1	0	1	1	3	5	0	0	2.6
MP 2 adults	250–530	8	21	16	12	0	0	0	0	0	0	6.9
MP 2 infants	250–530	27	22	9	0	0	19	0	2	0	0	1.9
MP 3 adults	350–550	13	35	68	0	2	9	2	43	0	0	12.2
MP 3 infants	350–550	24	4	19	5	0	2	0	6	14		2.1
MP 4 adults	500–700	8	0	17	0	0	1	0	0	0	0	2.25
MP4 infants	500–700	7	2	4	0	13	0	0	1	0	0	2.8
Eastern mound burials												
MP2 adults	150–530	5	4	35	14	2	0	1	0	0	0	11.2
MP2 infants	150–530	23	18	7	0	1	12	0	5	0	1	1.9
Totals		137	157	177	32	19	44	6	63	14	1	**513**

- Are these sources consistent with the known regional copper and lead producers?
- Can we detect variation within individual mortuary assemblages?
- Can we detect horizontal variation between mortuary assemblages of the same mortuary phase?
- Can we detect vertical variation between mortuary assemblages of different mortuary phases?
- Can we detect similarities in consumption signatures between NBJ and contemporary cemeteries in Thailand and Cambodia?

Methodology

X-ray fluorescence (XRF)

Bulk elemental composition of major, minor and (some) trace elements for the OM samples was analysed using XRF at the *Laboratoire Archéomatériaux et Prévision de l'Altération* (LAPA-IRAMAT/CEA) in Saclay, France. XRF data were acquired using a NITON XL 3t GOLDD+ portable XRF analyser in 'laboratory mode' (fixed stand but no vacuum), with a max 40 kV accelerating voltage in the 'alloys' mode. Accuracy and precision were assessed with eleven Certified Reference Materials (Table 3). Good results for major and minor components were confirmed but light elements at low concentrations like phosphorus, silicon, aluminium, magnesium and sulphur were not reliably detected due to non-vacuum conditions. Analyses were performed on the metal samples after resin-mounting, grinding with silicon carbide paper (from 800 to 4000 grits) and polishing using diamond suspensions (3, 1 and 0.25 µm). The mounted and polished sections were scanned using a 3 mm beam diameter, which allowed for reliable results if the sample was larger than this. Three such spot analyses were made for each sample.

Optical microscopy (OM)

The same samples as prepared for XRF analysis were examined for microstructural evidence of thermo-mechanical treatments using an optical microscope (Zeiss Imager A2 vario Axio system), first un-etched and then after etching with alcoholic ferric chloride, to reveal the crystalline structures in less corroded examples. The advanced corrosion of many of the NBJ copper-base artefacts means their microstructures could not be reliably read (Scott 1991). However, all those samples with unusual elemental compositions were examined, as well as a selection of other uncorroded or less-corroded examples to illustrate the range of working techniques evidenced.

Fig. 4 Copper-base artefacts from Non Ban Jak. Mortuary Phase 1. Cat. 350, burial 18, foetal infant, ring. Cat. 452, burial 30, infant, bracelet left wrist. Cat. 591, burial 35, old female, bracelet right wrist. Cat. 609, burial 59, anklet left ankle. Cat. 377, burial 20, old adult male, toe ring over left ankle. Cat. 371, burial 21, adult male, bracelet right wrist. Mortuary Phase 2. Cat. 879, burial 86, infant, bracelet placed over left wrist. Cat. 929, infant, bracelet worn on right wrist. Cat. 930, infant, bracelet worn on left wrist. Cat 941, infant, bracelet worn on left wrist. Cat. 1303, old male, finger ring on right hand. Cat. 1505. Young male, bracelet worn on right wrist. Cat. 1985, burial 190, old male, silver ring worn on right hand. Cat. 1302, burial 134, old male, toe ring worn on right foot. Cat. 1679, bell, phase 1 occupation. Cat. 1948, infant, bell beside skull. Cat. 1808, infant, on left arm. Cat. 1807, infant, on right arm. Cat. 1871, burial 177, infant, right arm. Cat. 1870, burial 177, infant, left arm

Scanning electron microscopy with energy dispersive spectrometry (SEM-EDS)

XRF/OM samples with unusual microstructures and/or elemental compositions were carbon coated for analysis in a JEOL 7001F instrument. Both secondary electron (SE) and backscattered electron (BSE) modes were used, with a 20 kV accelerating voltage, a 10 mm working distance with an Oxford Silicon Drift Detector and processed using Oxford Instruments Aztec software.

The detection limit was fixed at 0.5 wt.% with a count rate of 4000/s (detection time of 40 s), which gave good spectral resolution with respect to background noise. Relative quantification error (2 σ) is circa 10% of the measured value. SEM-EDS accuracy was evaluated using the same CRMs as used for the pXRF analysis, and we obtained good results for the major elements (Table 3). Bulk compositions for each sample were obtained by a mean of 3–4 areas scan ($0.4\ mm^2$) per sample. When possible, the analyses were performed in areas without corrosion products.

Multi collector – inductively coupled plasma – mass spectrometer (MC-ICP-MS)

Lead isotope analysis (LIA) was conducted at the *Service d'Analyse des Roches et des Minéraux* of the Centre for Petrographic and Geochemical Research (SARM-CRPG) in Nancy, France, using MC-ICP-MS after lead extraction (Manhes et al. 1980). Thallium NIST SRM 997 was used to correct for instrumental mass bias and all parameters were adjusted to obtain the closest values relative to NIST SRM 981, as determined by DS-TIMS (Thirlwall 2002). More details about SARM-CRPG lead isotope analysis are available in (Cloquet et al. 2006; Aebischer et al. 2015).

As per the SEALIP/BROGLASEA programmes, LIA was used to look for consistency/compatibility, not

Fig. 5 Copper-base artefacts from Non Ban Jak. Mortuary Phase 3. Cat. 1190, burial 120, mid adult male, bracelet right arm. Cat. 1191, burial 120, mid adult male, bracelet right wrist. Cat. 1197, burial 120, mid adult male, heavy ring between femora. Cat. 1193, burial 120, mid adult male, earring right ear. Cat. 1223, burial 122 infant, anklet. Cats. 839–840, burial 82, old male, belts. Cat. 512, burial 46 adult, toe ring left foot. Cat. 553, burial 46 adult, ring right hand. Cat. 514, burial 46 adult, anklet right foot. Cat. 725, burial 73 child, ring, right toe. Cat. 554, infant, burial 157, ring, necklace. Cat. 786, burial 77 old male right earring. Cat. 542, young male, bracelet right wrist. Cat. 713, burial 75 old female, bracelet right wrist. Cat. 1134, 15–18 year old, bracelet right wrist. Mortuary Phase 4. Cat 491, burial 39 infant bracelet right arm. Cat. 522, burial 45 old male, finger ring left hand. Cat. 635, burial 66 child, ear ring right ear. Cat. 669, burial 66 child, necklace ring. Cat. 1385, burial 110 young male, ring. Cat. 72. Burial 7 old female, ring, right hand. Cat. 78. Burial 7 old female, bracelet left hand. Cat. 334. Burial 12 old adult, spiral. Cat. 400. Burial 12 old adult, spiral. Cat. 613, burial 61a/b adult females, toe rings. Cat. 470. Burial 32, infant, belt

'matches', with known and characterised production systems, in recognition of the likelihood of other, as yet uncharacterised, primary and/or secondary production systems, as well as interpretation being impacted by mixing, alloying and recycling (Budd et al. 1993; Wilson and Pollard 2001; Pryce et al. 2011b, 2014). These consistencies were judged by proximity of data points on $^{208}Pb/^{204}Pb$

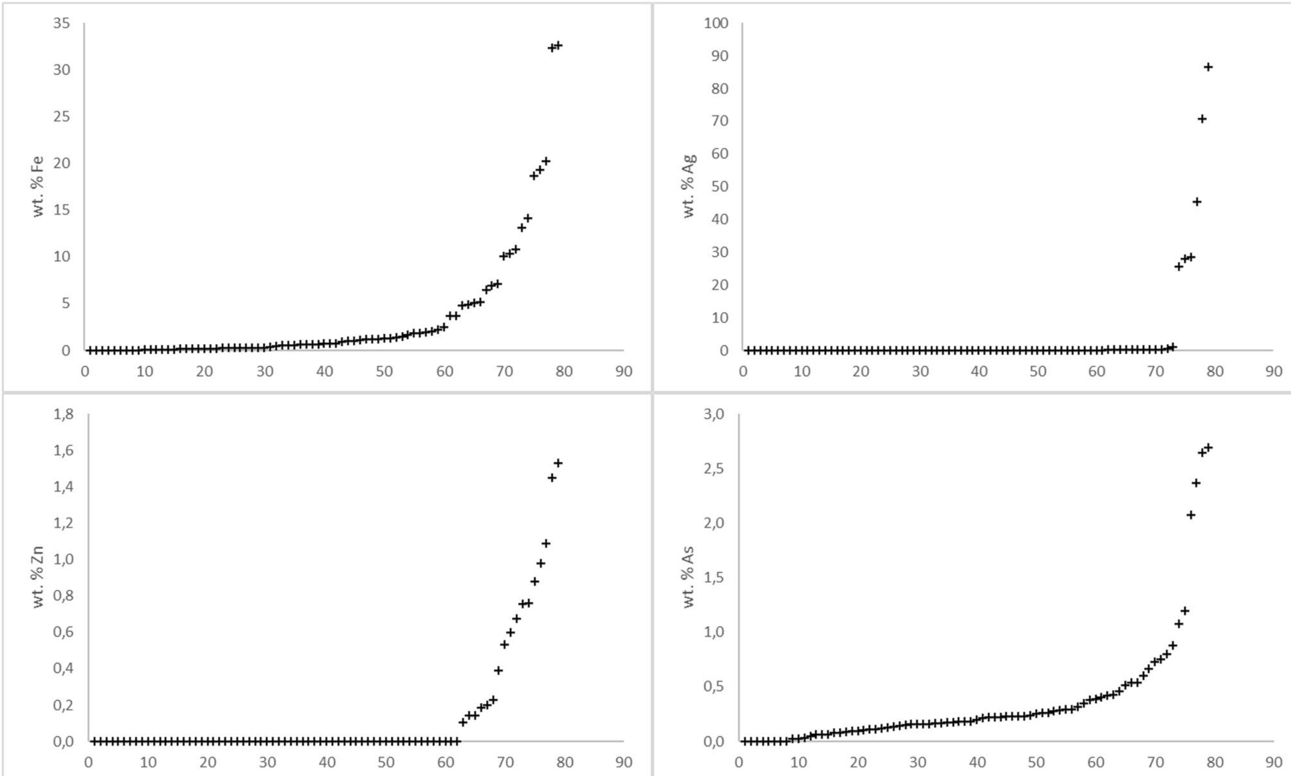

Fig. 6 NBJ samples sorted by elemental concentration, clockwise from top-left: iron, silver, zinc and arsenic

vs $^{206}Pb/^{204}Pb$ and $^{207}Pb/^{204}Pb$ vs $^{206}Pb/^{204}Pb$ biplots for manual interpretation.

Results

Elemental and technological

The advanced degree of corrosion in many NBJ samples implies our elemental data cannot be considered to represent the alloy compositions when the artefacts were originally produced (Scott 2002). This is particularly apparent in the generally elevated tin concentrations, ranging up to 45 wt. %, which would have been artificially inflated as the copper concentrations were depleted by preferential corrosion. Furthermore, the frequent and occasionally high concentrations of non-cuprophile minor oxides like iron, aluminium and silicon are corroborative of visually determined advanced corrosion products. Nevertheless, on a presence:absence basis (Bray and Pollard 2012), applying the standard BROGLASEA alloying element cutoff convention of 1 wt. %, we can discern the following alloy classes: 45 'bronzes'; 4 'leaded arsenical bronzes'; 1 'leaded arsenical silver copper', 1 'leaded arsenical gunmetal', 20 'leaded bronzes'; 2 'leaded gunmetal'; 1 'leaded silver bronze'; 1 'silver bronze', 3 'silver coppers' and 1 gunmetal. We do not imply that all these alloy classes were intentionally produced, and some are almost certainly conflated due to post-depositional modification of original values, but we can still detect significant patterning with respect to arsenic, iron, lead, silver, tin and zinc (Fig. 6).

Many of these alloy types are uncommon but none of the artefacts are made from a pure or near-pure metal. This is consistent, but not mutually exclusive, with NBJ not having any secondary production evidence, for which we might expect foundrypersons to have produced their own alloys from imported raw smelted copper, tin and lead. Of course, it would also be reasonable for putative foundrypersons to produce finished products from pre-alloyed metals, or simply by recycling whatever stock and scrap came their way, but on balance we favour the strictly-evidenced interpretation of all artefacts being imported to NBJ in their finished form.

Lead

Firstly, and critical to lead isotope data interpretation, 50 NBJ samples are 'unleaded', in terms of having global compositions lower than 1 wt.% Pb – from around 1400 to 7000

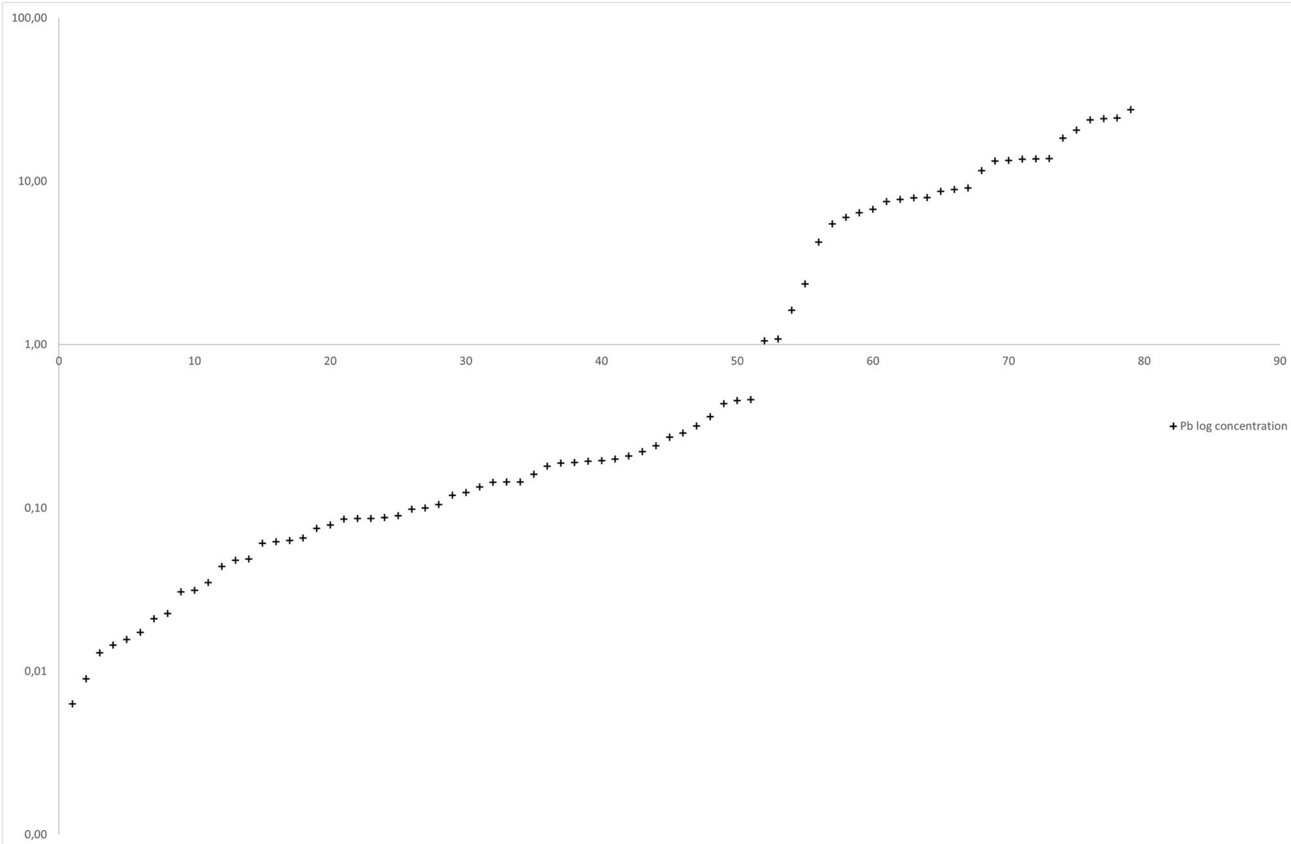

Fig. 7 Logarithmic lead concentrations for NBJ samples, showing our 1 wt.% Pb alloying boundary is reasonable and corresponds to a real gap in the data distribution

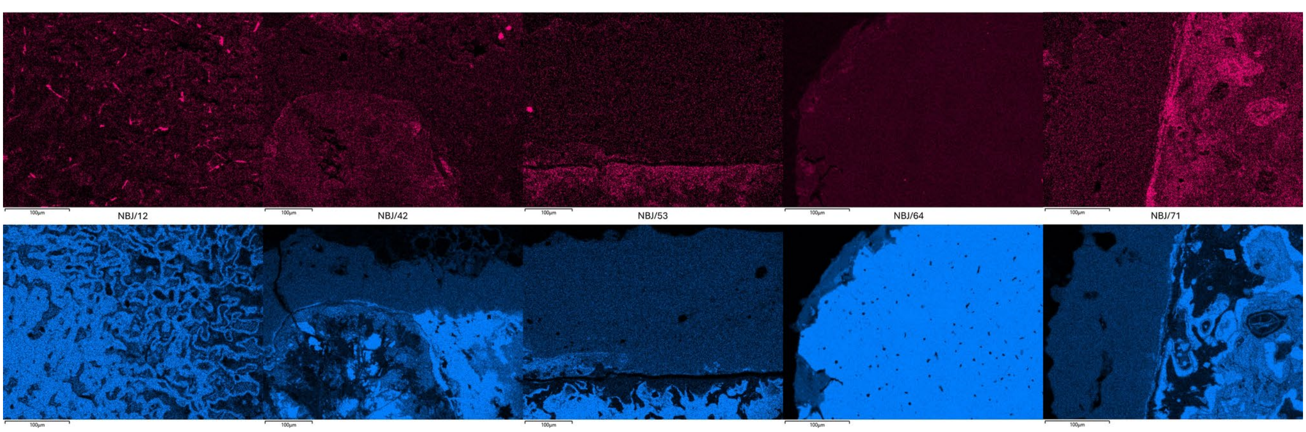

Fig. 8 SEM-EDS elemental mapping for the samples with more than 1 wt. % As, showing the non-surficial distribution of As (top) in Cu (bottom)

ppm – while the remaining 29 samples are 'leaded', with an extant 1.1 to 27.5 wt. % Pb. There is a distinct gap in the variation, suggesting our alloying boundary definition is historically as well as analytically useful in this instance (Fig. 7, see also Pryce et al. 2024). Lead concentration will prove a deciding factor in our isotopic interpretations.

Arsenic and zinc

We do not consider any of the four NBJ samples (#21, 41–42, 53) with global compositions above 1 wt.% Zn (Table 1) to be brasses. Indeed, their zinc concentrations are too low to be detected by SEM-EDS (Table 1). While deliberate

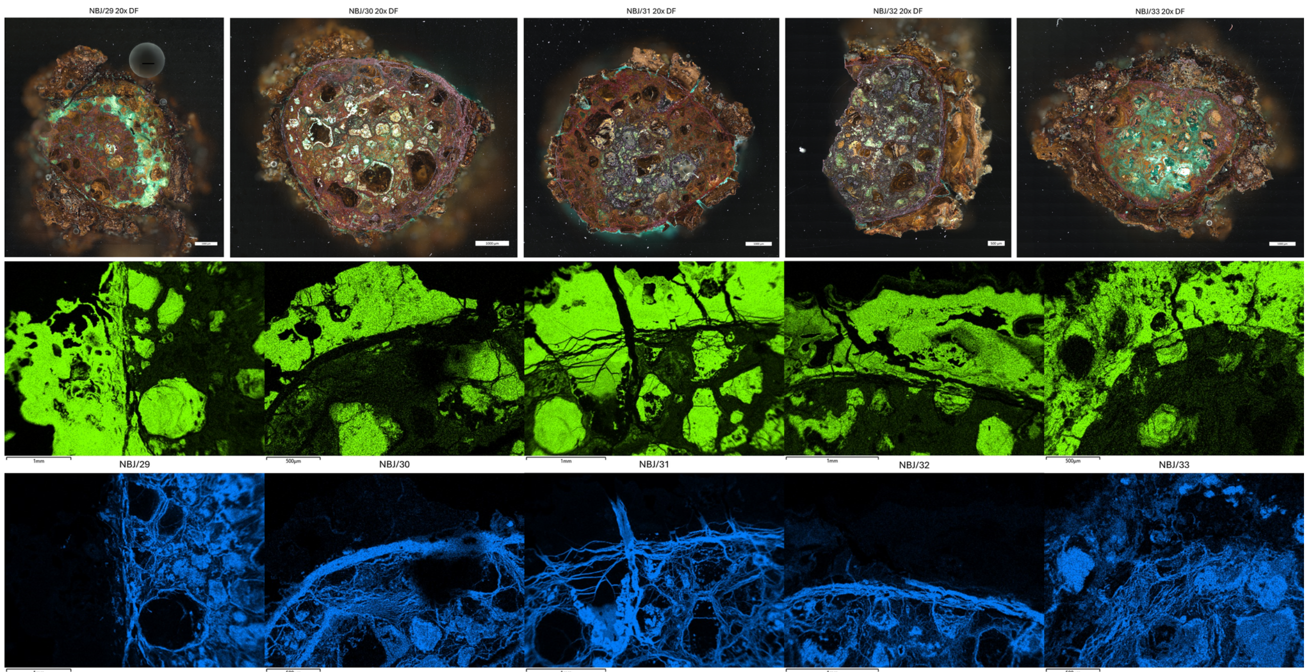

Fig. 9 (upper) Dark field optical micrographs of the NBJ samples with the high iron concentrations. (lower) SEM-EDS elemental maps for iron-rich samples NBJ/29–33, with Fe distributions highlighted in green above, and Cu in blue below

alloying, co-smelting or cementation are unlikely, it is conceivable these samples reflect lead-zinc (galena-sphalerite) mineralisations from west-central Thailand (Charusiri et al. 2003) or elsewhere in the region. Likewise, we do not interpret any of the 61 samples with globally-detectable arsenic, or the six samples with 1.1 to 2.7 wt. % As (#12–13, 53, 62, 64 & 71) to be true arsenical alloys (Table 1). Five of those six also contain significant tin contents, which would have given the colour and hardness properties that arsenic might otherwise have contributed, if arsenic had been alloyed intentionally for aesthetic or mechanical advantages. SEM-EDS analyses (Table 1) do confirm the presence of As at 1.0 to 4.2 wt.% but elemental mapping (Fig. 8) shows the arsenic is not (with the possible exception of NBJ/53, which is a complex leaded-arsenic-zinc-bronze) distributed in a surficial layer of a copper arsenide (Cu_3As), which can provide a desirable silver colour. We attribute the composition of these samples as most likely due to the unintentional presence of arsenic due to smelting or co-smelting arsenic-bearing copper minerals like arsenopyrite.

Iron

The 'bimetallic rings' were assumed by the excavators to have been made of bronze and iron due to their colour and mass, but we consider these are more likely corroded unleaded bronzes with unusually elevated global iron concentrations ranging from 1.8 to 32.6 wt. % Fe (Table 1, undoubtedly being more suited to a stoichiometric Fe_2O_3 conversion factor of 1.431). As above, we do not suggest these figures are quantitative representations of the original alloy, and indeed we see significant covariation with context: the samples with the most iron are NBJ/29–32, all of which came from Burial 167, and thus suggestive that a particular post-depositional environment maybe be partly responsible (Fig. 9). Of the Burial 177 bimetallics, NBJ/33–36, all have single-digit iron concentrations, with the exception of NBJ/33 (global, 19.4 wt.% Fe), and the two remaining 'bimetallic' samples from Burials 49 (NBJ/46, global 4.8 wt.% Fe) and 120 (NBJ/63, global 3.7 wt.% Fe), respectively, are likewise not so rich in iron to be seriously considered iron or partly-iron artefacts. We are as yet unable to explain the globular appearance of Cu versus Fe distributions in elemental mapping (Fig. 9) but strongly suspect tropical weathering processes over the centuries, in a manner similar to pisolithic laterite formation (see Pryce and Natapintu 2009; Venunan 2016, and geological references therein). The existence of copper-base artefacts with elevated iron concentrations is far from unknown, either elsewhere in Eurasia (Craddock and Meeks 1987; Ingo et al. 2006), or indeed in Southeast Asia (Cadet et al. 2019). The typical reason for the presence of iron in copper is excessively reducing conditions during the smelting of ferruginous copper ores and/or iron-rich fluxes. Iron can be easily removed from copper as dross in a hot oxidising atmosphere, and thus its presence in NBJ samples is most likely symptomatic of casting copper-base

Table 2 NBJ study samples coding, context, date and typology

Name	Burial	Cat#	MP	absolute period	Artefact type
SEALIP/TH/NBJ/1	B18	350	1	AD 200 - 400	bracelet
SEALIP/TH/NBJ/2	B18	350	1	AD 200 - 400	spiral bracelet
SEALIP/TH/NBJ/3	B20	377	1	AD 200 - 400	thumb ring
SEALIP/TH/NBJ/4	B21	371a	1	AD 200 - 400	bracelet
SEALIP/TH/NBJ/5	B21	371b	1	AD 200 - 400	bracelet
SEALIP/TH/NBJ/6	B21	371c	1	AD 200 - 400	bracelet
SEALIP/TH/NBJ/7	B30	452a	1	AD 200 - 400	flat ring
SEALIP/TH/NBJ/8	B30	452b	1	AD 200 - 400	ring
SEALIP/TH/NBJ/9	B30	452c	1	AD 200 - 400	ring
SEALIP/TH/NBJ/10	B35	591	1	AD 200 - 400	flat bracelet
SEALIP/TH/NBJ/11	B59	609	1	AD 200 - 400	flat bracelet
SEALIP/TH/NBJ/12	B86	879a	2	AD 400 - 550	bracelet
SEALIP/TH/NBJ/13	B86	879b	2	AD 400 - 550	bracelet
SEALIP/TH/NBJ/14	B90	929a	2	AD 400 - 550	flat bracelet
SEALIP/TH/NBJ/15	B90	929b	2	AD 400 - 550	flat bracelet
SEALIP/TH/NBJ/16	B90	929c	2	AD 400 - 550	flat bracelet
SEALIP/TH/NBJ/17	B90	930a	2	AD 400 - 550	flat bracelet
SEALIP/TH/NBJ/18	B90	930b	2	AD 400 - 550	flat bracelet
SEALIP/TH/NBJ/19	B90	930c	2	AD 400 - 550	flat bracelet
SEALIP/TH/NBJ/20	B91	941a	2	AD 400 - 550	flat bracelet
SEALIP/TH/NBJ/21	B91	941b	2	AD 400 - 550	flat bracelet
SEALIP/TH/NBJ/22	B134	1303a	2	AD 400 - 550	ring
SEALIP/TH/NBJ/23	B134	1303b	2	AD 400 - 550	ring
SEALIP/TH/NBJ/24	B134	1302a	2	AD 400 - 550	toe ring
SEALIP/TH/NBJ/25	B134	1302b	2	AD 400 - 550	toe ring
SEALIP/TH/NBJ/26	B134	1302c	2	AD 400 - 550	toe ring
SEALIP/TH/NBJ/27	B141	1355	2	AD 400-550	anklet
SEALIP/TH/NBJ/28	B147	1505	2	AD 400 - 550	large flat bracelet
SEALIP/TH/NBJ/29	B167	1807a	2	AD 400 - 550	bimetallic ring
SEALIP/TH/NBJ/30	B167	1807b	2	AD 400 - 550	bimetallic ring
SEALIP/TH/NBJ/31	B167	1808a	2	AD 400 - 550	bimetallic ring
SEALIP/TH/NBJ/32	B167	1808b	2	AD 400 - 550	bimetallic ring
SEALIP/TH/NBJ/33	B177	1870a	2	AD 400 - 550	bimetallic ring
SEALIP/TH/NBJ/34	B177	1870b	2	AD 400 - 550	bimetallic ring
SEALIP/TH/NBJ/35	B177	1871a	2	AD 400 - 550	bimetallic ring
SEALIP/TH/NBJ/36	B177	1871b	2	AD 400 - 550	bimetallic ring
SEALIP/TH/NBJ/37	B190	1985	2	AD 400 - 550	silver ring
SEALIP/TH/NBJ/38	B192	1948	2	AD 400 - 550	bell
SEALIP/TH/NBJ/39	N1 3:7	1679	2	AD 400 - 550	bell
SEALIP/TH/NBJ/40	B46	512a	3	AD 550 - 600	toe ring
SEALIP/TH/NBJ/41	B46	512b	3	AD 550 - 600	toe ring
SEALIP/TH/NBJ/42	B46	512c	3	AD 550 - 600	toe ring
SEALIP/TH/NBJ/43	B46	514a	3	AD 550 - 600	anklet
SEALIP/TH/NBJ/44	B46	514b	3	AD 550 - 600	anklet
SEALIP/TH/NBJ/45	B46	514c	3	AD 550 - 600	anklet
SEALIP/TH/NBJ/46	B49	553	3	AD 550 - 600	bimetallic ring
SEALIP/TH/NBJ/47	B49	554a	3	AD 550 - 600	ring
SEALIP/TH/NBJ/48	B49	554b	3	AD 550 - 600	ring
SEALIP/TH/NBJ/49	B49	554c	3	AD 550 - 600	ring
SEALIP/TH/NBJ/50	B49	542	3	AD 550 - 600	bracelet
SEALIP/TH/NBJ/51	B71	679	3	AD 550 - 600	bracelet

Table 2 (continued)

Name	Burial	Cat#	MP	absolute period	Artefact type
SEALIP/TH/NBJ/52	B72	752	3	AD 550-600	finger ring
SEALIP/TH/NBJ/53	B73	725	3	AD 550 - 600	toe ring
SEALIP/TH/NBJ/54	B75	713	3	AD 550 - 600	bracelet
SEALIP/TH/NBJ/55	B77	786	3	AD 550 - 600	earring
SEALIP/TH/NBJ/56	B82	839	3	AD 550 - 600	belt
SEALIP/TH/NBJ/57	B82	840	3	AD 550 - 600	belt
SEALIP/TH/NBJ/58	B114	1134a	3	AD 550 - 600	bracelet
SEALIP/TH/NBJ/59	B114	1134b	3	AD 550 - 600	bracelet
SEALIP/TH/NBJ/60	B120	1190	3	AD 550 - 600	bracelet (C-section)
SEALIP/TH/NBJ/61	B120	1191	3	AD 550 - 600	bracelet
SEALIP/TH/NBJ/62	B120	1193	3	AD 550 - 600	earring
SEALIP/TH/NBJ/63	B120	1197	3	AD 550 - 600	bimetallic ring
SEALIP/TH/NBJ/64	B122	1223	3	AD 550 - 600	bracelet
SEALIP/TH/NBJ/65	B39	491	4	AD 600 - 850	bracelet
SEALIP/TH/NBJ/66	B45	522a	4	AD 600 - 850	ring
SEALIP/TH/NBJ/67	B45	522b	4	AD 600 - 850	ring
SEALIP/TH/NBJ/68	B66	635	4	AD 600 - 850	ring
SEALIP/TH/NBJ/69	B66	669a	4	AD 600 - 850	ring
SEALIP/TH/NBJ/70	B66	669b	4	AD 600 - 850	ring
SEALIP/TH/NBJ/71	B66	669c	4	AD 600 - 850	ring
SEALIP/TH/NBJ/72	B110	1385	4	AD 600 - 850	ring
SEALIP/TH/NBJ/73	B7	72a	4	AD 600 - 850	ring
SEALIP/TH/NBJ/74	B7	72b	4	AD 600 - 850	ring
SEALIP/TH/NBJ/75	B7	78a	4	AD 600 - 850	bracelet
SEALIP/TH/NBJ/76	B12	334	4	AD 600 - 850	spiral
SEALIP/TH/NBJ/77	B12	400	4	AD 600 - 850	spiral
SEALIP/TH/NBJ/78	B32	470	4	AD 600 - 850	belt
SEALIP/TH/NBJ/79	B61a/b	613a	4	AD 600 - 850	ring
SEALIP/TH/NBJ/80	B61a/b	613b	4	AD 600 - 850	ring
SEALIP/TH/NBJ/81	B61a/b	613c	4	AD 600 - 850	ring

artefacts using unrefined copper. In this instance, this 'dirty bronze' may have been imported as batches for Burial 167 & 177 funerary rites.

Silver

A regionally-novel aspect of the NBJ assemblage is the presence of silver alloys, or significant traces of silver in 11 samples dated MP2 to MP4 (Tables 2 & 1). These have global silver concentrations ranging from 2000 ppm, with one sample (NBJ/22) having 1.1 wt. % Ag, and six (NBJ/37, 50, 61, 62, 65 & 72) having 25.8 to 86.5 wt. % Ag (Fig. 6). NBJ/22 is highly corroded (42.2 wt. % Sn & 1.2 wt.% Fe), so while silver is certainly detected, we consider it a 'bronze' rather than a silver alloy. However, the six samples with more than 25 wt. % Ag were examined by OM and SEM-EDS to tentatively explain their composition and fabrication (Fig. 10).

NBJ/37 (global 71.2 wt. % Ag, Table 1), a MP2 (AD 400 – 550) thin flat-section ring from Burial 190, is heavily corroded but appears to have a lamellar structure, consistent with it having been worked. The global composition also has 3 wt.% Sn and 1 wt. % Pb but curiously, no copper detected, which may be a result of post-depositional modification, as indicated by the 15 wt.% Cl. SEM-EDS area scan of the better-preserved core confirms a predominantly argentiferous phase,69 wt.% Ag, as well as the 1 wt.% Pb. However, the 3 wt.% Sn seen with XRF is below detection limit, whilst the copper missing in the bulk analysis appears at 1.2 wt.%. SEM-EDS elemental mapping does not help us to distinguish the dispersion of Ag and Cu in the sample (Fig. 10) and thus the ring's construction is unclear.

NBJ/50 (global 45.5 wt. % Ag, Table 1), an interrupted round-section bracelet from MP3 (AD 550 – 600) Burial 49, but with two macroscopically visible phases in section (Fig. 10), indicating that the XRF analysis is likely to be highly unrepresentative. Microscopically, the sample has an incomplete encirclement of corrosion, up to 1 mm thick, followed by a silvery phase up to 1 mm thick,

Table 3 CRMs for the present study, as analysed with pXRF, SEM-EDS and with certified values given. Data given to 1 d.p., *bdl* is below detection limit

Sample	Sb	Sn	Bi	Pb	Zn	Cu	Ni	Co	Fe	Mn	Al	S
B10 pXRF	1.2	7.2	*bdl*	4.1	2.9	83.2	1.1	*bdl*	0.2	*bdl*	*bdl*	*bdl*
B10 SEM-EDS	1.7	6.6	*bdl*	3.6	3.0	82.7	1.0	*bdl*	*bdl*	*bdl*	*bdl*	*bdl*
B10 certified value	1.1	7.0	0.0	4.1	2.8	83.7	1.0	0.0	0.2	0.0	0.2	0.0
B12 pXRF	0.1	10.1	*bdl*	0.2	0.7	85.2	2.8	*bdl*	0.2	0.2	*bdl*	*bdl*
B12 SEM-EDS	*bdl*	9.5	*bdl*	*bdl*	0.9	84.9	3.1	*bdl*	*bdl*	*bdl*	*bdl*	*bdl*
B12 certified value	0.1	9.6	0.0	0.2	0.6	85.7	2.6	0.0	0.2	0.2	0.1	0.0
51.13-4 pXRF	*bdl*	0.3	*bdl*	0.1	0.4	91.0	*bdl*	*bdl*	1.9	0.9	4.9	*bdl*
51.13-4 SEM-EDS	*bdl*	*bdl*	*bdl*	*bdl*	0.7	87.7	*bdl*	*bdl*	1.9	1.1	7.8	*bdl*
51.13-4 certified value	0.0	0.3	0.0	0.0	0.3	88.8	0.1	0.0	1.8	0.9	7.3	0.0
71.32-4 pXRF	0.3	6.4	*bdl*	4.3	7.1	80.5	0.8	*bdl*	0.4	*bdl*	*bdl*	*bdl*
71.32-4 SEM-EDS	*bdl*	6.4	*bdl*	3.1	7.3	81.8	0.8	*bdl*	0.4	*bdl*	*bdl*	*bdl*
71.32-4 certified value	0.3	6.5	0.1	4.4	6.5	80.5	0.7	0.0	0.4	0.1	0.1	0.0
SRM-500 pXRF	*bdl*	*bdl*	*bdl*	*bdl*	0.1	99.7	0.1	*bdl*	*bdl*	*bdl*	*bdl*	*bdl*
SRM-500 SEM-EDS	*bdl*	*bdl*	*bdl*	*bdl*	0.4	99.4	*bdl*	*bdl*	*bdl*	*bdl*	*bdl*	*bdl*
SRM-500 certified value	0.0	0.0	0.0	0.0	0.0	99.7	0.1	0.0	0.0	0.0	0.0	0.0
C1123 pXRF	*bdl*	*bdl*	*bdl*	*bdl*	*bdl*	97.4	*bdl*	2.5	*bdl*	*bdl*	*bdl*	*bdl*
C1123 SEM-EDS	*bdl*	*bdl*	*bdl*	*bdl*	*bdl*	96.5	*bdl*	3.4	*bdl*	*bdl*	*bdl*	*bdl*
C1123 certified value	0.0	0.0	0.0	0.0	0.0	97.4	0.0	2.3	0.0	0.0	0.0	0.0
SRM1275 pXRF	*bdl*	*bdl*	*bdl*	*bdl*	*bdl*	86.9	10.7	*bdl*	1.6	0.4	*bdl*	*bdl*
SRM1275 SEM-EDS	*bdl*	*bdl*	*bdl*	*bdl*	*bdl*	87.9	10.1	*bdl*	1.5	0.5	*bdl*	*bdl*
SRM1275 certified value	0.0	0.0	0.0	0.0	0.1	88.2	9.8	0.0	1.5	0.4	0.0	0.0
L-20-1 pXRF	*bdl*	0.5	*bdl*	0.3	14.4	84.2	0.2	*bdl*	*bdl*	0.1	*bdl*	*bdl*
L-20-1 SEM-EDS	*bdl*	0.5	*bdl*	*bdl*	14.6	84.0	*bdl*	*bdl*	*bdl*	*bdl*	*bdl*	*bdl*
L-20-1 certified value	0.0	0.5	0.0	0.3	13.3	85.2	0.2	0.0	0.0	0.1	0.1	0.0
B21 pXRF	0.2	5.3	*bdl*	3.7	6.5	82.2	1.3	*bdl*	0.3	*bdl*	*bdl*	*bdl*
B21 SEM-EDS	*bdl*	5.2	*bdl*	3.9	7.0	82.2	1.3	*bdl*	*bdl*	*bdl*	*bdl*	*bdl*
B21 certified value	0.2	5.1	0.0	3.8	6.2	83.0	1.2	0.0	0.3	0.0	0.1	0.0
B31 pXRF	0.5	8.0	*bdl*	10.6	0.8	79.4	0.6	*bdl*	*bdl*	*bdl*	*bdl*	*bdl*
B31 SEM-EDS	1.8	8.0	*bdl*	9.9	1.1	78.6	0.5	*bdl*	*bdl*	*bdl*	*bdl*	*bdl*
B31 certified value	0.5	7.7	0.0	11.8	0.8	78.6	0.5	0.0	0.0	0.0	0.0	0.0
UZ-52-3 pXRF	0.1	1.0	*bdl*	0.1	18.0	80.3	0.1	*bdl*	0.3	*bdl*	*bdl*	*bdl*
UZ-52-3 SEM-EDS	*bdl*	1.0	*bdl*	*bdl*	18.2	80.2	*bdl*	*bdl*	*bdl*	*bdl*	*bdl*	*bdl*
UZ-52-3 certified value	0.1	1.1	0.0	0.1	17.0	81.1	0.1	0.0	0.3	0.0	0.0	0.0

and finally a coppery core up to 2.5 mm in diameter. All uncorroded phases are cored and as-cast, with the silvery-to-coppery boundary irregular but distinct. SEM-EDS area scans of the silver-rich outer phase give highly comparable data, with Cu concentrations giving way to Ag as expected (Table 1). NBJ/50 offers no sign of the silvery layer having been attached mechanically, as in a foil or leaf, and detailed manual examination of the XRF spectra did not reveal any mercury peaks, which might indicate amalgam silvering. Thus immersion or depletion silvering remain the intentional options, versus a very deep and regular post-depositional corrosion.

NBJ/61 (global, 86.5 wt. % Ag, Table 1), a MP3 (AD 550 – 600) interrupted round-section bracelet from Burial 120, has a largely mono-alloy as-cast microstructure, with some post-depositional corrosion phase of up to 300 µm around half the perimeter (Fig. 10). SEM-EDS area scan of the core indicates a reduced silver concentration of 57.8 wt.% (Table 1), with a greater proportion of copper (15.8 vs 10.3 wt.%), similar of lead (0.3 vs 0.2 wt.%), while tin is no longer detected (0.9 vs 0.0 wt.%). The SEM-EDS detection of silicon and chlorine suggests post-depositional corrosion has had an impact throughout the sample. These factors suggest NBJ/61's constituent metal was alloyed fully and allowed to cool slowly in the mould.

NBJ/62 (global, 28.7 wt. % Ag, 66.3 wt. % Cu, Table 1), a MP3 earring from burial 120, has two macroscopically-visible phases: a copper-rich core of 1.5–2 mm diameter, with a copper-depleted perimeter 0.5 – 1 mm thick (Fig. 10). SEM-EDS area scan of the core highlights the higher copper concentration of 70.1 wt.%, with correspondingly decreased silver at 24.3 wt.%, and lead and arsenic concentrations

Table 4 Normalised elemental data with working totals for the NBJ artefacts, indicating analysis method and probable alloy. Pd, Ru, Mo, Nb & Co scanned for but not detected, bdl is below detection limit

Name	Artefact type	O	Sb	Sn	Cd	Ag	Zr	Bi	Pb	Se	As	Au	W	Zn	Cu	Ni	Fe	Mn	Cr	V	Ti	Al	S	Cl	P	Si	Mg	total	Technique	Alloy
SEALIP/TH/NBJ/1	bracelet	bdl	bdl	28.2	bdl	bdl	bdl	bdl	0.1	bdl	0.2	bdl	bdl	bdl	67.5	bdl	0.3	bdl	bdl	bdl	bdl	bdl	bdl	bdl	0.1	3.6	bdl	100.0	pXRF	bronze
SEALIP/TH/NBJ/2	spiral bracelet	bdl	0.2	35.4	bdl	bdl	bdl	bdl	0.2	bdl	0.2	bdl	bdl	bdl	62.2	bdl	1.0	bdl	bdl	bdl	bdl	bdl	bdl	bdl	bdl	0.7	bdl	100.0	pXRF	bronze
SEALIP/TH/NBJ/3	thumb ring	bdl	0.1	27.2	bdl	bdl	bdl	bdl	bdl	bdl	0.1	bdl	bdl	bdl	71.6	0.1	0.1	bdl	bdl	bdl	0.2	bdl	0.1	bdl	bdl	0.4	bdl	100.1	pXRF	bronze
SEALIP/TH/NBJ/4	bracelet	bdl	0.4	37.9	bdl	0.3	bdl	bdl	0.2	bdl	0.1	bdl	bdl	bdl	56.4	bdl	3.7	bdl	bdl	bdl	bdl	bdl	bdl	bdl	0.1	0.7	bdl	99.9	pXRF	bronze
SEALIP/TH/NBJ/5	bracelet	bdl	0.2	17.4	bdl	bdl	bdl	bdl	0.1	bdl	0.1	bdl	bdl	bdl	65.3	bdl	10.1	bdl	bdl	bdl	bdl	bdl	bdl	bdl	0.3	6.5	bdl	100.0	pXRF	bronze
SEALIP/TH/NBJ/6	bracelet	bdl	0.3	28.6	bdl	0.3	bdl	bdl	0.2	bdl	0.1	bdl	bdl	bdl	67.9	bdl	1.9	bdl	bdl	bdl	0.2	bdl	bdl	bdl	0.1	0.5	bdl	100.1	pXRF	bronze
SEALIP/TH/NBJ/7	flat ring	bdl	bdl	18.3	bdl	bdl	bdl	bdl	0.1	bdl	0.1	bdl	bdl	bdl	73.2	bdl	5.1	bdl	bdl	bdl	bdl	bdl	bdl	bdl	bdl	3.3	bdl	100.0	pXRF	bronze
SEALIP/TH/NBJ/8	ring	bdl	0.3	24.0	bdl	bdl	bdl	bdl	0.1	bdl	0.1	bdl	bdl	bdl	73.1	bdl	0.5	bdl	bdl	bdl	bdl	bdl	bdl	bdl	0.1	1.9	bdl	100.0	pXRF	bronze
SEALIP/TH/NBJ/9	ring	bdl	0.3	24.3	bdl	0.4	bdl	bdl	0.1	bdl	0.1	bdl	bdl	bdl	72.8	bdl	1.7	bdl	bdl	bdl	bdl	bdl	bdl	bdl	bdl	0.2	bdl	100.0	pXRF	bronze
SEALIP/TH/NBJ/10	flat bracelet	bdl	0.2	33.7	bdl	0.2	bdl	bdl	2.4	bdl	0.1	bdl	bdl	bdl	62.6	bdl	0.3	bdl	bdl	bdl	bdl	bdl	bdl	bdl	bdl	0.4	bdl	100.0	pXRF	leaded bronze
SEALIP/TH/NBJ/11	flat bracelet	bdl	0.1	28.0	bdl	bdl	bdl	bdl	0.4	bdl	bdl	bdl	bdl	bdl	69.3	bdl	1.3	bdl	bdl	bdl	bdl	bdl	bdl	bdl	0.1	0.9	bdl	100.0	pXRF	bronze
SEALIP/TH/NBJ/12	bracelet	bdl	0.2	14.8	bdl	0.3	bdl	0.3	6.4	bdl	2.7	bdl	bdl	bdl	72.9	bdl	0.7	bdl	bdl	bdl	0.1	bdl	bdl	bdl	bdl	1.5	bdl	100.0	pXRF	leaded arsenical bronze

Table 4 (continued)

Name	Artefact type	O	Sb	Sn	Cd	Ag	Zr	Bi	Pb	Se	As	Au	W	Zn	Cu	Ni	Fe	Mn	Cr	V	Ti	Al	S	Cl	P	Si	Mg	total	Technique	Alloy
SEALIP/TH/NBJ/13	bracelet	bdl	0.2	11.1	bdl	0.3	bdl	0.2	7.5	bdl	2.1	bdl	bdl	bdl	68.4	0.1	0.7	bdl	bdl	bdl	bdl	bdl	bdl	bdl	bdl	9.4	bdl	99.8	pXRF	leaded arsenical bronze
SEALIP/TH/NBJ/14	flat bracelet	bdl	bdl	6.0	bdl	bdl	bdl	bdl	bdl	bdl	0.1	bdl	bdl	bdl	64.2	bdl	18.7	bdl	bdl	bdl	bdl	bdl	bdl	bdl	0.1	10.8	bdl	100.0	pXRF	bronze
SEALIP/TH/NBJ/15	flat bracelet	bdl	0.2	22.0	bdl	bdl	bdl	bdl	0.1	bdl	0.2	bdl	bdl	bdl	70.6	0.1	6.5	bdl	bdl	bdl	bdl	bdl	bdl	bdl	bdl	0.4	bdl	100.0	pXRF	bronze
SEALIP/TH/NBJ/16	flat bracelet	bdl	bdl	25.1	bdl	0.2	bdl	bdl	0.1	bdl	0.2	bdl	bdl	bdl	66.9	0.1	4.9	bdl	bdl	bdl	bdl	bdl	0.2	bdl	bdl	2.3	bdl	100.0	pXRF	bronze
SEALIP/TH/NBJ/17	flat bracelet	bdl	bdl	21.7	bdl	bdl	bdl	bdl	0.1	bdl	0.2	bdl	bdl	0.2	61.6	0.1	14.1	bdl	bdl	bdl	bdl	bdl	0.2	bdl	0.1	1.8	bdl	100.0	pXRF	bronze
SEALIP/TH/NBJ/18	flat bracelet	bdl	bdl	21.6	bdl	bdl	bdl	bdl	0.1	bdl	0.2	bdl	bdl	0.2	65.7	0.1	10.8	bdl	bdl	bdl	bdl	bdl	0.2	bdl	0.1	1.1	bdl	100.0	pXRF	bronze
SEALIP/TH/NBJ/19	flat bracelet	bdl	bdl	24.4	bdl	bdl	bdl	bdl	0.1	bdl	0.2	bdl	bdl	0.8	62.1	bdl	10.4	bdl	bdl	bdl	bdl	bdl	0.2	bdl	bdl	1.8	bdl	100.0	pXRF	bronze
SEALIP/TH/NBJ/20	flat bracelet	bdl	bdl	22.3	bdl	bdl	bdl	bdl	0.2	bdl	0.3	bdl	bdl	0.6	66.5	bdl	6.9	bdl	bdl	bdl	bdl	bdl	bdl	bdl	bdl	3.2	bdl	99.9	pXRF	bronze
SEALIP/TH/NBJ/21	flat bracelet	bdl	bdl	20.5	bdl	bdl	bdl	bdl	0.1	bdl	0.2	bdl	0.2	1.1	64.4	bdl	7.1	bdl	bdl	bdl	bdl	bdl	0.3	bdl	bdl	6.0	bdl	100.0	pXRF	zinc bronze
SEALIP/TH/NBJ/22	ring	bdl	1.5	42.2	bdl	1.1	bdl	bdl	0.2	bdl	0.1	bdl	bdl	bdl	53.0	bdl	1.2	bdl	bdl	bdl	bdl	bdl	bdl	bdl	bdl	0.6	bdl	100.0	pXRF	bronze
SEALIP/TH/NBJ/23	ring	bdl	0.9	24.2	bdl	bdl	bdl	bdl	0.1	bdl	bdl	bdl	bdl	bdl	73.3	bdl	0.6	bdl	bdl	bdl	bdl	bdl	bdl	bdl	bdl	0.7	bdl	100.0	pXRF	bronze
SEALIP/TH/NBJ/24	toe ring	bdl	0.3	18.1	bdl	bdl	bdl	bdl	0.1	bdl	0.1	bdl	bdl	bdl	66.9	bdl	0.7	bdl	bdl	bdl	bdl	bdl	bdl	bdl	0.1	13.7	bdl	100.0	pXRF	bronze
SEALIP/TH/NBJ/25	toe ring	bdl	0.4	21.9	bdl	0.3	bdl	bdl	0.1	bdl	0.1	bdl	bdl	bdl	75.9	0.1	0.2	bdl	bdl	bdl	bdl	bdl	bdl	bdl	bdl	0.9	bdl	100.0	pXRF	bronze

Table 4 (continued)

Name	Artefact type	O	Sb	Sn	Cd	Ag	Zr	Bi	Pb	Se	As	Au	W	Zn	Cu	Ni	Fe	Mn	Cr	V	Ti	Al	S	Cl	P	Si	Mg	total	Technique	Alloy
SEALIP/TH/NBJ/26	toe ring	bdl	0.5	33.2	bdl	bdl	bdl	bdl	0.1	bdl	0.1	bdl	bdl	bdl	62.9	bdl	1.0	bdl	bdl	bdl	bdl	bdl	bdl	bdl	bdl	2.1	bdl	100.0	pXRF	bronze
SEALIP/TH/NBJ/27	-	-	-	-	-	-	-	-	-	-	-	-	-	-	-	-	-	-	-	-	-	-	-	-	-	-	-	-	-	-
SEALIP/TH/NBJ/28	large flat bracelet	bdl	bdl	10.2	bdl	bdl	bdl	0.1	0.7	bdl	bdl	0.3	bdl	bdl	82.7	bdl	0.3	0.1	bdl	bdl	bdl	bdl	2.6	bdl	1.3	1.7	bdl	65.3	pXRF	bronze
SEALIP/TH/NBJ/29	bimetallic ring	bdl	bdl	14.9	bdl	bdl	bdl	bdl	bdl	bdl	0.2	bdl	bdl	bdl	50.7	0.1	32.6	bdl	bdl	bdl	bdl	bdl	0.2	bdl	0.1	1.1	bdl	100.0	pXRF	bronze
SEALIP/TH/NBJ/30	bimetallic ring	bdl	0.1	28.1	bdl	bdl	bdl	bdl	0.1	bdl	0.3	bdl	bdl	bdl	51.4	0.2	19.3	bdl	bdl	bdl	bdl	bdl	bdl	bdl	0.1	0.3	bdl	99.9	pXRF	bronze
SEALIP/TH/NBJ/31	bimetallic ring	bdl	bdl	18.0	bdl	bdl	bdl	bdl	bdl	bdl	0.2	bdl	bdl	bdl	60.6	0.2	20.2	bdl	bdl	bdl	bdl	bdl	0.2	bdl	0.1	0.5	bdl	100.0	pXRF	bronze
SEALIP/TH/NBJ/32	bimetallic ring	bdl	0.1	15.3	bdl	bdl	bdl	bdl	bdl	bdl	0.1	bdl	bdl	bdl	49.7	0.2	32.4	0.2	bdl	bdl	bdl	bdl	0.2	bdl	0.3	1.5	bdl	100.0	pXRF	bronze
SEALIP/TH/NBJ/33	bimetallic ring	bdl	0.1	22.3	bdl	bdl	bdl	bdl	bdl	bdl	0.3	bdl	0.1	bdl	54.9	0.1	19.4	bdl	bdl	bdl	bdl	bdl	0.5	bdl	0.2	2.3	bdl	67.7	pXRF	bronze
SEALIP/TH/NBJ/34	bimetallic ring	bdl	bdl	36.3	bdl	bdl	bdl	bdl	bdl	bdl	0.4	bdl	0.1	bdl	59.5	bdl	2.8	bdl	bdl	bdl	0.1	bdl	0.3	bdl	bdl	0.4	bdl	64.2	pXRF	bronze
SEALIP/TH/NBJ/35	bimetallic ring	bdl	0.1	29.4	bdl	bdl	bdl	bdl	0.1	bdl	0.3	bdl	0.1	bdl	61.8	bdl	7.1	bdl	bdl	bdl	bdl	bdl	0.3	bdl	0.1	0.6	bdl	72.7	pXRF	bronze
SEALIP/TH/NBJ/36	bimetallic ring	bdl	0.1	35.5	bdl	bdl	bdl	bdl	bdl	bdl	0.6	bdl	0.1	bdl	59.1	0.1	3.0	bdl	bdl	bdl	0.1	bdl	0.4	bdl	0.1	0.8	bdl	67.7	pXRF	bronze
SEALIP/TH/NBJ/37	silver ring	7.8	bdl	3.2	bdl	71.2	bdl	bdl	1.1	bdl	bdl	bdl	bdl	bdl	bdl	bdl	bdl	bdl	bdl	bdl	bdl	0.9	bdl	15.1	bdl	0.8	bdl	99.3	SEM-EDS	leaded silver bronze
SEALIP/TH/NBJ/38	bell	bdl	bdl	13.1	bdl	bdl	bdl	0.1	24.2	bdl	bdl	0.1	bdl	0.9	53.2	bdl	0.3	bdl	bdl	bdl	bdl	1.9	bdl	bdl	bdl	6.2	bdl	100.1	pXRF	leaded bronze

Table 4 (continued)

Name	Artefact type	O	Sb	Sn	Cd	Ag	Zr	Bi	Pb	Se	As	Au	W	Zn	Cu	Ni	Fe	Mn	Cr	V	Ti	Al	S	Cl	P	Si	Mg	total	Technique	Alloy
SEALIP/TH/NBJ/39	bell	bdl	0.1	4.8	bdl	bdl	bdl	bdl	2.8	bdl	1.3	bdl	0.2	0.9	70.5	bdl	0.7	bdl	bdl	bdl	0.1	bdl	5.9	bdl	0.3	5.7	6.7	16.6	pXRF	leaded bronze
SEALIP/TH/NBJ/40	toe ring	3.5	bdl	10.4	bdl	bdl	bdl	bdl	18.4	bdl	0.5	bdl	bdl	bdl	65.8	bdl	bdl	bdl	bdl	bdl	bdl	bdl	bdl	1.3	bdl	bdl	bdl	100.1	SEM-EDS	leaded bronze
SEALIP/TH/NBJ/41	toe ring	bdl	bdl	6.0	bdl	bdl	bdl	0.1	13.6	bdl	bdl	bdl	0.2	1.0	69.3	bdl	0.5	bdl	bdl	bdl	bdl	1.4	bdl	bdl	bdl	7.8	bdl	100.3	pXRF	leaded zinc bronze
SEALIP/TH/NBJ/42	toe ring	bdl	bdl	6.7	bdl	bdl	bdl	bdl	13.8	bdl	bdl	bdl	0.4	1.5	73.6	bdl	0.2	bdl	bdl	bdl	bdl	bdl	bdl	bdl	bdl	3.7	bdl	99.5	pXRF	leaded zinc bronze
SEALIP/TH/NBJ/43	anklet	bdl	0.2	37.7	bdl	bdl	bdl	bdl	0.1	bdl	0.5	0.1	bdl	bdl	59.5	bdl	1.3	bdl	bdl	bdl	bdl	bdl	0.2	bdl	bdl	0.4	bdl	100.0	pXRF	bronze
SEALIP/TH/NBJ/44	anklet	bdl	0.1	20.8	bdl	bdl	bdl	bdl	0.1	bdl	0.7	0.1	bdl	bdl	77.2	bdl	0.2	bdl	bdl	bdl	bdl	bdl	bdl	bdl	0.1	0.6	bdl	100.0	pXRF	bronze
SEALIP/TH/NBJ/45	anklet	bdl	0.1	29.9	bdl	0.3	bdl	bdl	0.2	bdl	0.6	0.1	bdl	bdl	66.3	bdl	0.3	bdl	bdl	bdl	bdl	bdl	bdl	bdl	bdl	2.0	bdl	100.0	pXRF	bronze
SEALIP/TH/NBJ/46	bimetallic ring	bdl	0.2	33.7	bdl	bdl	bdl	bdl	0.2	bdl	0.4	bdl	bdl	bdl	60.5	0.2	4.8	bdl	bdl	bdl	bdl	bdl	bdl	bdl	bdl	bdl	bdl	100.0	pXRF	bronze
SEALIP/TH/NBJ/47	ring	bdl	bdl	8.6	bdl	bdl	bdl	0.1	8.7	bdl	0.8	0.1	bdl	0.2	71.1	bdl	0.6	bdl	bdl	bdl	bdl	bdl	bdl	bdl	bdl	9.9	bdl	99.7	pXRF	leaded bronze
SEALIP/TH/NBJ/48	ring	10.7	bdl	12.7	bdl	bdl	bdl	bdl	27.5	bdl	0.8	bdl	bdl	bdl	45.2	bdl	bdl	bdl	bdl	bdl	bdl	bdl	bdl	2.9	bdl	0.1	bdl	99.9	SEM-EDS	leaded bronze
SEALIP/TH/NBJ/49	ring	bdl	bdl	8.8	bdl	bdl	0.1	0.1	7.7	bdl	0.5	0.1	bdl	bdl	63.5	bdl	1.4	bdl	bdl	bdl	bdl	1.2	bdl	bdl	bdl	16.7	bdl	100.1	pXRF	leaded bronze
SEALIP/TH/NBJ/50	bracelet	bdl	0.1	2.2	bdl	45.5	bdl	0.1	0.4	bdl	0.2	0.3	bdl	bdl	51.2	0.1	bdl	bdl	bdl	bdl	bdl	bdl	bdl	bdl	bdl	bdl	bdl	99.9	pXRF	silver-bronze
SEALIP/TH/NBJ/51	bracelet	bdl	0.2	14.9	bdl	bdl	bdl	0.1	7.9	bdl	0.4	bdl	bdl	bdl	76.2	bdl	0.1	bdl	bdl	bdl	0.1	bdl	bdl	bdl	bdl	bdl	bdl	99.7	pXRF	leaded bronze

Table 4 (continued)

Name	Artefact type	O	Sb	Sn	Cd	Ag	Zr	Bi	Pb	Se	As	Au	W	Zn	Cu	Ni	Fe	Mn	Cr	V	Ti	Al	S	Cl	P	Si	Mg	total	Technique	Alloy
SEALIP/TH/NBJ/52																														
SEALIP/TH/NBJ/53	toe ring	bdl	bdl	13.2	bdl	bdl	bdl	0.3	5.3	0.1	2.1	bdl	3.4	1.3	56.6	0.2	2.0	bdl	0.5	0.3	0.2	1.3	bdl	bdl	bdl	13.2	bdl	113.7	pXRF	*leaded arsenical zinc bronze*
SEALIP/TH/NBJ/54	bracelet	bdl	0.2	9.9	bdl	bdl	bdl	0.1	8.9	bdl	0.3	bdl	bdl	bdl	80.4	0.1	bdl	bdl	bdl	bdl	0.1	bdl	bdl	bdl	bdl	bdl	bdl	100.0	pXRF	leaded bronze
SEALIP/TH/NBJ/55	earring	bdl	0.2	1.9	bdl	bdl	bdl	0.2	4.2	bdl	0.7	bdl	bdl	bdl	92.4	0.1	bdl	bdl	bdl	bdl	bdl	bdl	bdl	bdl	bdl	0.3	bdl	100.0	pXRF	leaded bronze
SEALIP/TH/NBJ/56	belt	bdl	0.2	36.9	bdl	0.4	bdl	bdl	0.2	bdl	0.2	bdl	bdl	bdl	60.1	bdl	1.2	bdl	bdl	bdl	bdl	bdl	bdl	bdl	bdl	0.8	bdl	100.0	pXRF	bronze
SEALIP/TH/NBJ/57	belt	bdl	0.1	34.4	bdl	bdl	bdl	bdl	0.1	bdl	0.5	bdl	0.1	bdl	62.0	bdl	0.8	bdl	bdl	bdl	bdl	bdl	0.9	bdl	bdl	1.0	bdl	64.4	pXRF	bronze
SEALIP/TH/NBJ/58	bracelet	bdl	0.2	9.2	bdl	bdl	bdl	0.1	8.0	bdl	0.5	bdl	bdl	bdl	81.6	bdl	0.3	bdl	bdl	bdl	0.1	bdl	bdl	bdl	bdl	bdl	bdl	100.0	pXRF	leaded bronze
SEALIP/TH/NBJ/59	bracelet	bdl	0.1	9.5	bdl	bdl	bdl	0.1	11.6	bdl	bdl	bdl	bdl	bdl	78.4	0.1	0.1	bdl	bdl	bdl	bdl	bdl	bdl	bdl	bdl	0.2	bdl	100.0	pXRF	leaded bronze
SEALIP/TH/NBJ/60	bracelet (C-section)	bdl	0.2	14.2	bdl	bdl	bdl	0.1	13.5	bdl	0.4	bdl	bdl	bdl	71.5	bdl	0.1	bdl	bdl	bdl	bdl	bdl	bdl	bdl	bdl	bdl	bdl	99.1	pXRF	leaded bronze
SEALIP/TH/NBJ/61	bracelet	bdl	bdl	0.9	bdl	86.5	bdl	bdl	0.3	bdl	bdl	0.2	bdl	bdl	10.3	bdl	0.2	bdl	bdl	bdl	bdl	bdl	bdl	bdl	bdl	1.6	bdl	100.0	pXRF	silver-copper
SEALIP/TH/NBJ/62	earring	bdl	bdl	0.0	bdl	28.7	bdl	0.2	1.1	bdl	1.1	bdl	bdl	bdl	66.3	bdl	0.2	bdl	bdl	bdl	bdl	bdl	bdl	bdl	bdl	2.3	bdl	99.8	pXRF	leaded arsenical silver copper
SEALIP/TH/NBJ/63	bimetallic ring	bdl	bdl	32.1	bdl	bdl	bdl	bdl	bdl	bdl	0.2	bdl	bdl	bdl	62.8	0.2	3.7	bdl	bdl	bdl	bdl	bdl	0.2	bdl	0.1	0.5	bdl	100.0	pXRF	bronze

Table 4 (continued)

Name	Artefact type	O	Sb	Sn	Cd	Ag	Zr	Bi	Pb	Se	As	Au	W	Zn	Cu	Ni	Fe	Mn	Cr	V	Ti	Al	S	Cl	P	Si	Mg	total	Technique	Alloy
SEALIP/TH/NBJ/64	bracelet	bdl	0.1	5.6	bdl	0.2	bdl	bdl	1.6	bdl	2.6	0.1	bdl	bdl	89.4	0.1	0.3	bdl	bdl	bdl	bdl	bdl	bdl	bdl	bdl	bdl	bdl	100.0	pXRF	leaded arsenical bronze
SEALIP/TH/NBJ/65	bracelet	bdl	bdl	0.6	bdl	27.9	bdl	0.1	0.3	bdl	0.2	0.2	bdl	bdl	70.3	bdl	bdl	bdl	bdl	bdl	bdl	bdl	bdl	bdl	bdl	0.3	bdl	100.0	pXRF	silver-copper
SEALIP/TH/NBJ/66	ring	bdl	bdl	8.0	bdl	bdl	0.1	0.1	6.8	bdl	0.4	0.1	bdl	0.1	59.6	bdl	1.5	bdl	bdl	bdl	bdl	1.3	bdl	bdl	bdl	21.9	bdl	99.5	pXRF	leaded bronze
SEALIP/TH/NBJ/67	ring	bdl	bdl	4.3	bdl	bdl	0.1	0.1	5.5	bdl	0.2	bdl	0.1	0.5	49.7	bdl	1.2	bdl	bdl	bdl	bdl	3.0	bdl	bdl	bdl	35.3	bdl	100.0	pXRF	leaded bronze
SEALIP/TH/NBJ/68	ring	bdl	bdl	8.0	bdl	bdl	0.1	bdl	13.3	bdl	bdl	0.1	bdl	bdl	52.8	bdl	1.1	bdl	bdl	bdl	bdl	3.0	bdl	bdl	bdl	21.5	bdl	100.0	pXRF	leaded bronze
SEALIP/TH/NBJ/69	ring	bdl	bdl	9.3	bdl	bdl	0.1	0.2	24.4	bdl	bdl	0.2	bdl	0.8	56.4	bdl	0.2	bdl	bdl	bdl	bdl	1.7	bdl	bdl	bdl	6.8	bdl	100.2	pXRF	leaded bronze
SEALIP/TH/NBJ/70	ring	bdl	bdl	8.8	bdl	bdl	bdl	0.1	9.1	bdl	0.3	0.1	bdl	0.1	62.4	bdl	0.6	bdl	bdl	bdl	bdl	0.6	bdl	bdl	bdl	17.8	bdl	99.5	pXRF	leaded bronze
SEALIP/TH/NBJ/71	ring	12.3	bdl	14.4	bdl	bdl	bdl	bdl	20.3	bdl	1.2	bdl	bdl	bdl	46.9	bdl	0.1	bdl	bdl	bdl	bdl	bdl	bdl	4.9	bdl	0.1	bdl	101.7	SEM-EDS	leaded arsenical bronze
SEALIP/TH/NBJ/72	ring	bdl	bdl	0.0	bdl	25.8	bdl	bdl	0.3	bdl	0.3	bdl	bdl	0.4	69.3	bdl	0.4	bdl	0.1	bdl	bdl	bdl	bdl	bdl	bdl	3.4	bdl	99.9	pXRF	silver-copper
SEALIP/TH/NBJ/73	ring	11.2	bdl	12.3	bdl	bdl	bdl	bdl	23.8	bdl	0.9	bdl	bdl	bdl	49.8	bdl	bdl	bdl	bdl	bdl	bdl	bdl	0.3	1.7	bdl	bdl	bdl	100.0	SEM-EDS	leaded bronze
SEALIP/TH/NBJ/74	ring	bdl	bdl	7.7	bdl	bdl	bdl	0.1	13.7	bdl	0.3	0.1	bdl	0.7	63.1	bdl	0.6	bdl	bdl	0.1	0.1	2.1	bdl	bdl	bdl	11.4	bdl	100.6	pXRF	leaded bronze
SEALIP/TH/NBJ/75	bracelet	bdl	0.1	31.3	bdl	bdl	bdl	bdl	0.2	bdl	0.4	bdl	bdl	bdl	67.1	bdl	0.8	bdl	bdl	bdl	0.1	bdl	bdl	bdl	bdl	bdl	bdl	99.9	pXRF	bronze
SEALIP/TH/NBJ/76	spiral	bdl	0.2	25.9	0.1	bdl	bdl	bdl	0.1	bdl	0.4	bdl	0.1	bdl	60.9	0.1	4.3	0.1	bdl	bdl	0.1	bdl	1.9	bdl	0.2	5.7	bdl	45.4	pXRF	bronze

Table 4 (continued)

Name	Artefact type	O	Sb	Sn	Cd	Ag	Zr	Bi	Pb	Se	As	Au	W	Zn	Cu	Ni	Fe	Mn	Cr	V	Ti	Al	S	Cl	P	Si	Mg	total	Tech-nique	Alloy
SEALIP/TH/NBJ/77	spiral	bdl	0.1	20.6	bdl	bdl	bdl	bdl	0.1	bdl	0.3	bdl	0.1	bdl	64.4	bdl	4.1	bdl	bdl	bdl	bdl	bdl	1.4	bdl	0.3	8.4	bdl	60.6	pXRF	bronze
SEALIP/TH/NBJ/78	belt	bdl	0.1	18.3	0.1	bdl	bdl	bdl	bdl	bdl	0.2	bdl	0.3	bdl	69.5	bdl	0.2	bdl	bdl	bdl	0.1	bdl	1.2	bdl	0.3	9.7	bdl	17.2	pXRF	bronze
SEALIP/TH/NBJ/79	ring	bdl	0.1	19.4	0.1	bdl	bdl	bdl	0.1	bdl	0.2	bdl	0.2	bdl	66.1	bdl	1.0	bdl	bdl	bdl	0.1	bdl	0.4	bdl	0.2	12.1	bdl	31.3	pXRF	bronze
SEALIP/TH/NBJ/80	ring	bdl	0.1	28.5	bdl	bdl	bdl	bdl	0.1	bdl	0.4	bdl	0.2	bdl	67.7	bdl	0.3	bdl	bdl	bdl	bdl	bdl	0.2	bdl	bdl	2.4	bdl	74.3	pXRF	bronze
SEALIP/TH/NBJ/81	ring	bdl	0.2	44.9	bdl	bdl	bdl	bdl	0.2	bdl	0.2	bdl	bdl	bdl	52.9	bdl	1.0	bdl	bdl	bdl	bdl	bdl	bdl	bdl	bdl	0.6	bdl	100.0	pXRF	bronze

stable (Table 1). The microstructure is cored, indicating the artefact was left as-cast, while the diffuse and irregular boundary between the two major phases, seen optically and in elemental mapping (Fig. 10), suggests that post-depositional corrosion may be responsible for depleting copper concentrations from the outside in.

NBJ/65 (global, 27.9 wt.% Ag, 70.3 wt.% Cu, Table 1), a MP4 bracelet from burial 39, also has two predominant phases, a copper-rich centre 1.5 – 3 mm in diameter, with an irregular outer layer up to 300 µm thick. The cored dendrites throughout indicate the bracelet was left as-cast, and SEM-EDS analyses of the outer phase (30.7 wt.% Ag, 63.4 wt.% Cu, Table 1) suggest the phasing is due to post-depositional corrosion (Fig. 10). Likewise, NBJ/72 (global, 25.8 wt.% Ag, 69.3 wt. % Cu, Table 1), a MP4 square-section ring from burial 110, has two main phases, a copper-rich core about 1.2 mm per side, with an irregular copper-poor layer up to 150 µm thick (42.9 wt.% Ag, 49.4 wt.% Cu, Table 1, Fig. 16). The cored microstructure indicates the ring was left as-cast, meaning the square-section of the ring was achieved by casting or is not a real feature, while the irregular copper-depletion boundary suggests post-depositional corrosion produced the apparent phasing.

We will pursue the production techniques of these artefacts in a future paper but for the purposes of raw materials and provenance, we are inclined to view the above five artefacts as true silver-copper alloys, probably of varying Ag-Cu ratios when produced, which have been exacerbated by corrosion. Unfortunately, almost nothing is known about MSEA silver production, and certainly no prehistoric production centres are recorded, so while we might assume cupellation of silver from (extensive) regional lead deposits (Charusiri et al. 2003), we cannot assume a correlation of silver and lead concentrations; as seen in four of the NBJ samples with trace silver, and only two of the silver-rich samples, being 'leaded'. We certainly do not have the quality of elemental data achieved by Schlosser et al. (2012) in their study of gold and silver alloys at Prohear, a Mid-Iron Age (ca. 200 BC to AD 100) site in southeastern Cambodia, ca. 550 km and at least three centuries earlier than Non Ban Jak. They were able to look at Pt, Ir, Bi concentrations and the Pd/Pt ratio, which we cannot but we do note that of the 16 NBJ samples with detectable gold concentrations (500 to 2500 ppm), the three highest values corresponded to the samples (SEALIP/TH/NBJ/50,61,65) with substantial silver concentrations. This suggests electrum placer deposits in association with cassiterite may have been exploited but this is highly confused by the presence of copper and lead in the same samples.

In summary, the NBJ copper-base assemblage seems to reflect a pool of mixed and potentially recycled imported alloys, all of which were reasonably adapted to ornamental applications (Table 6).

Table 5 SEM-EDS global elemental composition data for samples with unusual alloy compositions. Data are normalised (analytical totals, 100%) and bdl is below detection limit. Alloys are indicated with elements in brackets if concentrations near the 1 wt.% alloy threshold

Name	Object	Alloy	O	Al	Si	S	Cl	Fe	Ni	Cu	Zn	As	Ag	Sn	Sb	Au	Pb	Bi	Total
SEALIP/TH/NBJ/29	ring	Fe	27.5	bdl	0.7	0.1	0.7	12.4	0.3	37.5	bdl	0.3	bdl	20.3	0.1	bdl	0.1	bdl	100
SEALIP/TH/NBJ/30	ring	Fe	25.9	bdl	1.7	0.1	1.8	22.5	0.4	33.2	bdl	0.5	bdl	13.7	bdl	bdl	0.1	bdl	100
SEALIP/TH/NBJ/31	ring	Fe	26.8	0.1	1.3	bdl	1.0	29.9	0.5	28.5	bdl	0.3	bdl	11.6	bdl	bdl	0.1	bdl	100
SEALIP/TH/NBJ/32	ring	Fe	21.7	bdl	0.5	0.3	0.3	18.0	0.4	34.2	bdl	0.3	bdl	24.1	0.3	bdl	0.1	bdl	100
SEALIP/TH/NBJ/33	ring	Fe	27.9	bdl	1.0	0.3	3.4	15.6	0.2	32.1	bdl	0.3	bdl	18.7	0.3	bdl	0.1	bdl	100
SEALIP/TH/NBJ/34	ring	Fe	20.5	bdl	0.5	0.2	8.8	2.1	bdl	39.2	bdl	0.2	bdl	28.0	0.2	bdl	0.2	bdl	100
SEALIP/TH/NBJ/35	ring	Fe	18.6	bdl	0.6	0.1	2.3	5.3	0.1	48.7	bdl	0.2	bdl	23.8	0.2	bdl	0.2	bdl	100
SEALIP/TH/NBJ/36	ring	Fe	18.3	bdl	0.8	0.2	2.8	2.9	0.1	40.2	bdl	0.4	bdl	33.6	0.4	bdl	0.1	bdl	100
SEALIP/TH/NBJ/37	ring	(Pb) Ag	8.2	1.3	2.4	bdl	17.0	0.2	bdl	1.2	bdl	0.1	68.6	bdl	bdl	bdl	1.0	bdl	100
SEALIP/TH/NBJ/50	bangle	Ag	12.0	bdl	1.5	0.1	0.7	0.1	bdl	36.2	bdl	0.2	46.9	1.8	bdl	0.1	0.5	bdl	100
SEALIP/TH/NBJ/61	bangle	Ag	18.7	0.3	5.6	0.1	1.1	0.2	bdl	15.8	bdl	0.1	57.8	bdl	bdl	bdl	0.2	bdl	100
SEALIP/TH/NBJ/62	ear-ring	Ag & As	1.6	bdl	0.1	bdl	1.7	bdl	bdl	70.1	bdl	1.2	24.3	bdl	bdl	0.1	0.9	bdl	100
SEALIP/TH/NBJ/65	bangle	Ag	2.5	bdl	0.1	bdl	2.2	bdl	0.1	63.4	bdl	0.2	30.7	0.2	bdl	0.2	0.4	bdl	100
SEALIP/TH/NBJ/72	ring	Ag	3.6	bdl	0.2	0.1	1.9	bdl	bdl	49.4	bdl	0.6	42.9	0.6	bdl	0.2	0.5	bdl	100
SEALIP/TH/NBJ/12	bangle	(Pb) As	1.6	bdl	0.2	0.3	0.4	0.7	0.1	75.1	bdl	3.8	0.3	14.8	0.4	0.1	2.0	0.3	100
SEALIP/TH/NBJ/13	bangle	(Pb) As	2.3	bdl	0.1	0.3	0.4	0.7	0.1	75.5	bdl	3.5	0.2	14.2	0.4	0.1	1.9	0.3	100
SEALIP/TH/NBJ/53	toe ring	(Pb) As & Zn	22.5	0.3	18.8	0.2	1.3	0.2	bdl	42.9	bdl	1.0	0.1	5.9	bdl	bdl	6.9	bdl	100
SEALIP/TH/NBJ/64	bangle	(Pb) As	1.5	bdl	0.2	0.2	1.1	0.3	bdl	85.0	bdl	4.2	0.3	5.5	0.2	0.2	1.2	0.2	100

Table 5 (continued)

Name	Object	Alloy	O	Al	Si	S	Cl	Fe	Ni	Cu	Zn	As	Ag	Sn	Sb	Au	Pb	Bi	Total
SEALIP/TH/NBJ/71	ring	(Pb) As	8.4	bdl	0.2	0.3	3.9	0.7	0.1	60.1	bdl	1.3	bdl	16.8	0.4	0.1	7.4	0.1	100
SEALIP/TH/NBJ/21	bangle	Zn	21.4	bdl	0.7	0.1	2.8	4.3	0.1	33.8	bdl	0.5	bdl	35.6	0.5	bdl	0.2	bdl	100
SEALIP/TH/NBJ/41	toe ring	(Pb) Zn	3.2	bdl	0.1	0.4	2.0	0.1	0.1	70.9	bdl	0.4	0.2	10.6	0.4	0.2	11.4	bdl	100
SEALIP/TH/NBJ/42	toe ring	(Pb) Zn	8.1	bdl	0.7	1.0	7.3	bdl	bdl	4.4	bdl	bdl	0.8	bdl	0.3	0.0	76.0	1.6	100

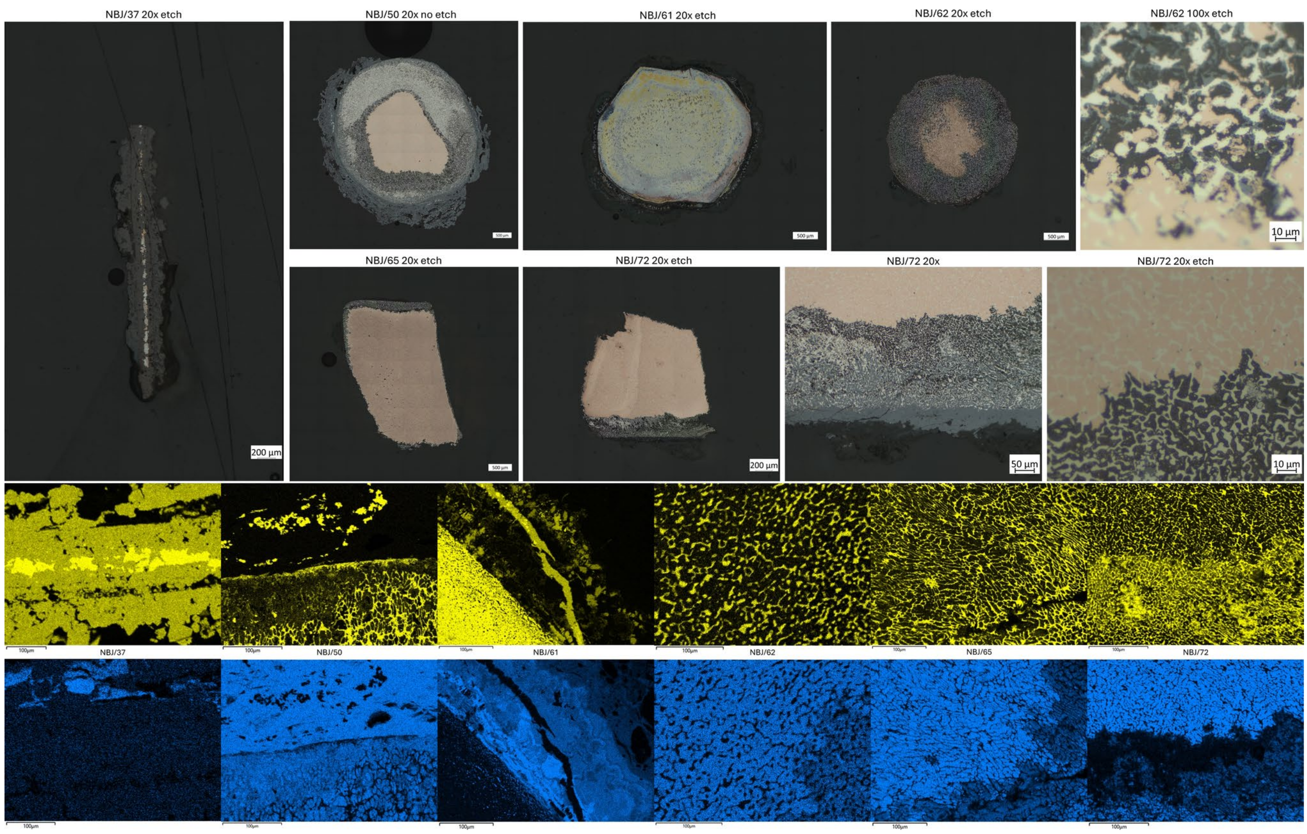

Fig. 10 (upper) Reflected light micrographs of samples NBJ/37, 50, 61, 62, 65 & 72, with details of the silver-rich and copper-rich phase interface for NBJ/62 & 72. (lower) SEM-EDS elemental maps for copper-rich/silver-rich samples NBJ/37, 50, 61, 62, 65 & 72, with Ag distributions highlighted in yellow above, and Cu in light blue below

Lead isotopic

As can be seen in Fig. 11, the NBJ copper-base assemblage LI data distribution is not homogeneous. It does have some clustering potentially indicative of multiple raw material sources but even with individual samples labelled, the patterning is not readily identifiable. The presence of LI clustering is to be expected from a large and typo-compositionally varied sample population from a long-lived site. Nevertheless, some order can be brought to the data by plotting the samples by mortuary phase (Fig. 12). This shows a clear but not absolute distinction between mortuary phases 1 and 2, and 3 and 4, which could be interpreted as metal supply networks shifting during the 6th c. AD.

Table 6 Raw measured lead isotope ratios for the studied NBJ samples (#27 & #52 no data)

Name	$^{206}Pb/^{204}Pb$	err (2σ)	$^{207}Pb/^{204}Pb$	err (2σ)	$^{208}Pb/^{204}Pb$	err (2σ)	$^{207}Pb/^{206}Pb$	err (2σ)	$^{206}Pb/^{207}Pb$	err (2σ)	$^{208}Pb/^{206}Pb$	err (2σ)
SEALIP/TH/NBJ/1	18.3694	0.003	15.7069	0.003	38.8666	0.008	0.8551	0.00002	1.1694	0.00002	2.1160	0.00016
SEALIP/TH/NBJ/2	18.3595	0.002	15.7164	0.002	38.8336	0.007	0.8561	0.00001	1.1681	0.00001	2.1152	0.00022
SEALIP/TH/NBJ/3	18.3752	0.003	15.7077	0.003	38.8416	0.010	0.8550	0.00002	1.1696	0.00002	2.1140	0.00026
SEALIP/TH/NBJ/4	18.3005	0.002	15.7624	0.002	38.6230	0.007	0.8613	0.00002	1.1610	0.00002	2.1105	0.00023
SEALIP/TH/NBJ/5	18.3033	0.003	15.7598	0.003	38.6184	0.009	0.8612	0.00002	1.1612	0.00002	2.1101	0.00015
SEALIP/TH/NBJ/6	18.3071	0.003	15.7560	0.003	38.6404	0.008	0.8608	0.00002	1.1618	0.00002	2.1108	0.00027
SEALIP/TH/NBJ/7	18.3323	0.002	15.7358	0.002	38.7103	0.006	0.8585	0.00001	1.1648	0.00001	2.1117	0.00018
SEALIP/TH/NBJ/8	18.3472	0.003	15.7448	0.003	38.7216	0.008	0.8583	0.00001	1.1651	0.00001	2.1105	0.00016
SEALIP/TH/NBJ/9	18.3461	0.005	15.7492	0.006	38.7092	0.018	0.8586	0.00001	1.1647	0.00001	2.1100	0.00051
SEALIP/TH/NBJ/10	18.3258	0.004	15.6864	0.004	38.8625	0.010	0.8561	0.00002	1.1681	0.00002	2.1208	0.00018
SEALIP/TH/NBJ/11	18.2666	0.003	15.7648	0.003	38.5575	0.007	0.8632	0.00001	1.1584	0.00001	2.1108	0.00017
SEALIP/TH/NBJ/12	18.3902	0.001	15.7175	0.001	38.8449	0.004	0.8549	0.00001	1.1698	0.00001	2.1123	0.00012
SEALIP/TH/NBJ/13	18.3921	0.002	15.7197	0.002	38.8508	0.006	0.8549	0.00002	1.1698	0.00002	2.1123	0.00012
SEALIP/TH/NBJ/14	18.3699	0.002	15.7250	0.002	38.8133	0.006	0.8562	0.00001	1.1680	0.00001	2.1129	0.00014
SEALIP/TH/NBJ/15	18.3651	0.002	15.7180	0.002	38.8398	0.008	0.8560	0.00001	1.1683	0.00001	2.1149	0.00022
SEALIP/TH/NBJ/16	18.3729	0.003	15.7265	0.003	38.8291	0.009	0.8561	0.00001	1.1681	0.00001	2.1135	0.00023
SEALIP/TH/NBJ/17	18.3733	0.003	15.7289	0.003	38.8279	0.008	0.8562	0.00002	1.1679	0.00002	2.1133	0.00020
SEALIP/TH/NBJ/18	18.3698	0.004	15.7240	0.004	38.8202	0.012	0.8561	0.00001	1.1680	0.00001	2.1133	0.00028
SEALIP/TH/NBJ/19	18.3709	0.004	15.7279	0.004	38.8323	0.010	0.8563	0.00002	1.1678	0.00002	2.1138	0.00021
SEALIP/TH/NBJ/20	18.3736	0.002	15.7180	0.002	38.8529	0.004	0.8555	0.00001	1.1689	0.00001	2.1148	0.00007
SEALIP/TH/NBJ/21	18.3736	0.002	15.7197	0.002	38.8530	0.005	0.8556	0.00002	1.1688	0.00002	2.1148	0.00007
SEALIP/TH/NBJ/22	18.3114	0.002	15.7624	0.002	38.6417	0.004	0.8608	0.00001	1.1616	0.00001	2.1103	0.00007
SEALIP/TH/NBJ/23	18.3071	0.002	15.7576	0.002	38.6262	0.007	0.8608	0.00001	1.1617	0.00001	2.1100	0.00020
SEALIP/TH/NBJ/24	18.3071	0.002	15.7510	0.002	38.6353	0.006	0.8605	0.00001	1.1621	0.00001	2.1105	0.00018
SEALIP/TH/NBJ/25	18.3041	0.002	15.7466	0.002	38.6520	0.007	0.8604	0.00001	1.1622	0.00001	2.1119	0.00014
SEALIP/TH/NBJ/26	18.3144	0.002	15.7541	0.002	38.6600	0.004	0.8603	0.00001	1.1624	0.00001	2.1110	0.00008
SEALIP/TH/NBJ/28	18.3761	0.002	15.7122	0.002	38.9071	0.005	0.8551	0.00001	1.1695	0.00001	2.1173	0.00010
SEALIP/TH/NBJ/29	18.4187	0.002	15.7163	0.002	38.8451	0.006	0.8533	0.00001	1.1719	0.00001	2.1090	0.00017
SEALIP/TH/NBJ/30	18.3306	0.002	15.7378	0.003	38.7265	0.010	0.8586	0.00001	1.1647	0.00001	2.1128	0.00031
SEALIP/TH/NBJ/31	18.4534	0.001	15.7193	0.001	38.8789	0.003	0.8518	0.00002	1.1740	0.00002	2.1070	0.00007
SEALIP/TH/NBJ/32	18.3320	0.001	15.7406	0.001	38.6946	0.003	0.8588	0.00002	1.1644	0.00002	2.1108	0.00006
SEALIP/TH/NBJ/33	18.3554	0.001	15.7360	0.002	38.7316	0.004	0.8575	0.00002	1.1662	0.00002	2.1102	0.00006
SEALIP/TH/NBJ/34	18.4784	0.001	15.7056	0.001	38.9135	0.003	0.8501	0.00003	1.1763	0.00003	2.1060	0.00005
SEALIP/TH/NBJ/35	18.3184	0.001	15.7181	0.001	38.7740	0.003	0.8579	0.00002	1.1657	0.00002	2.1167	0.00006
SEALIP/TH/NBJ/36	18.3409	0.001	15.7442	0.001	38.6989	0.003	0.8582	0.00003	1.1652	0.00003	2.1100	0.00008
SEALIP/TH/NBJ/37	18.2403	0.001	15.7454	0.001	38.4880	0.004	0.8636	0.00003	1.1580	0.00003	2.1101	0.00007
SEALIP/TH/NBJ/38	18.2793	0.001	15.7495	0.001	38.5823	0.003	0.8617	0.00001	1.1606	0.00001	2.1107	0.00006

Table 6 (continued)

Name	$^{206}Pb/^{204}Pb$	err (2σ)	$^{207}Pb/^{204}Pb$	err (2σ)	$^{208}Pb/^{204}Pb$	err (2σ)	$^{207}Pb/^{206}Pb$	err (2σ)	$^{206}Pb/^{207}Pb$	err (2σ)	$^{208}Pb/^{206}Pb$	err (2σ)
SEALIP/TH/NBJ/39	18.3611	0.001	15.7010	0.001	38.8796	0.003	0.8553	0.00001	1.1692	0.00001	2.1175	0.00006
SEALIP/TH/NBJ/40	18.3296	0.001	15.6789	0.001	38.8918	0.003	0.8557	0.00002	1.1686	0.00002	2.1218	0.00007
SEALIP/TH/NBJ/41	18.2225	0.001	15.6543	0.001	38.7911	0.003	0.8585	0.00002	1.1648	0.00002	2.1288	0.00009
SEALIP/TH/NBJ/42	18.2228	0.001	15.6540	0.001	38.7907	0.003	0.8584	0.00001	1.1649	0.00001	2.1287	0.00006
SEALIP/TH/NBJ/43	18.3790	0.001	15.7043	0.001	38.9094	0.003	0.8538	0.00001	1.1712	0.00001	2.1171	0.00008
SEALIP/TH/NBJ/44	18.3677	0.001	15.6929	0.001	38.9042	0.003	0.8538	0.00002	1.1713	0.00002	2.1181	0.00007
SEALIP/TH/NBJ/45	18.3594	0.001	15.6936	0.001	38.9063	0.003	0.8543	0.00001	1.1706	0.00001	2.1192	0.00008
SEALIP/TH/NBJ/46	18.3553	0.001	15.7342	0.001	38.7595	0.002	0.8574	0.00001	1.1664	0.00001	2.1117	0.00006
SEALIP/TH/NBJ/47	18.3726	0.001	15.7006	0.001	38.8931	0.002	0.8547	0.00002	1.1700	0.00002	2.1169	0.00005
SEALIP/TH/NBJ/48	18.4075	0.001	15.6982	0.001	38.9655	0.003	0.8529	0.00002	1.1725	0.00002	2.1169	0.00005
SEALIP/TH/NBJ/49	18.4034	0.001	15.7040	0.001	38.9306	0.003	0.8534	0.00001	1.1718	0.00001	2.1154	0.00005
SEALIP/TH/NBJ/50	18.2933	0.001	15.7046	0.001	38.7100	0.002	0.8584	0.00001	1.1650	0.00001	2.1161	0.00008
SEALIP/TH/NBJ/51	18.3518	0.001	15.6873	0.002	38.9018	0.004	0.8547	0.00002	1.1700	0.00002	2.1198	0.00010
SEALIP/TH/NBJ/53	18.3903	0.001	15.7061	0.001	38.9065	0.003	0.8540	0.00002	1.1709	0.00002	2.1157	0.00007
SEALIP/TH/NBJ/54	18.3906	0.001	15.6978	0.001	38.9404	0.004	0.8535	0.00003	1.1717	0.00003	2.1174	0.00010
SEALIP/TH/NBJ/55	18.4519	0.001	15.7137	0.001	38.9760	0.002	0.8517	0.00002	1.1742	0.00002	2.1124	0.00006
SEALIP/TH/NBJ/56	18.3700	0.001	15.7066	0.001	38.8644	0.003	0.8555	0.00002	1.1689	0.00002	2.1157	0.00007
SEALIP/TH/NBJ/57	18.3708	0.001	15.7025	0.001	38.8759	0.003	0.8553	0.00002	1.1692	0.00002	2.1162	0.00007
SEALIP/TH/NBJ/58	18.3933	0.001	15.6916	0.002	38.9164	0.004	0.8536	0.00002	1.1715	0.00002	2.1159	0.00010
SEALIP/TH/NBJ/59	18.3786	0.001	15.6844	0.001	38.9357	0.004	0.8539	0.00002	1.1711	0.00002	2.1185	0.00009
SEALIP/TH/NBJ/60	18.3493	0.001	15.6922	0.001	38.8490	0.003	0.8557	0.00002	1.1686	0.00002	2.1173	0.00009
SEALIP/TH/NBJ/61	18.2830	0.001	15.7373	0.001	38.5857	0.004	0.8613	0.00002	1.1611	0.00002	2.1106	0.00008
SEALIP/TH/NBJ/62	18.4695	0.001	15.7081	0.001	38.9892	0.004	0.8510	0.00002	1.1751	0.00002	2.1110	0.00010
SEALIP/TH/NBJ/63	18.4288	0.001	15.7094	0.001	38.8427	0.003	0.8529	0.00002	1.1724	0.00002	2.1077	0.00008
SEALIP/TH/NBJ/64	18.3975	0.001	15.6984	0.001	38.9060	0.004	0.8538	0.00002	1.1712	0.00002	2.1148	0.00006
SEALIP/TH/NBJ/65	18.3776	0.001	15.6944	0.001	38.8857	0.003	0.8545	0.00002	1.1703	0.00002	2.1159	0.00008
SEALIP/TH/NBJ/66	18.3893	0.001	15.7055	0.001	38.8805	0.003	0.8545	0.00002	1.1702	0.00002	2.1143	0.00008
SEALIP/TH/NBJ/67	18.3804	0.001	15.6847	0.001	38.9299	0.003	0.8538	0.00002	1.1712	0.00002	2.1181	0.00007
SEALIP/TH/NBJ/68	18.3745	0.001	15.6865	0.001	38.9250	0.003	0.8542	0.00002	1.1707	0.00002	2.1184	0.00007
SEALIP/TH/NBJ/69	18.3516	0.001	15.6852	0.001	38.8838	0.004	0.8552	0.00002	1.1693	0.00002	2.1188	0.00008
SEALIP/TH/NBJ/70	18.3732	0.001	15.6852	0.001	38.9114	0.004	0.8542	0.00002	1.1707	0.00002	2.1178	0.00009
SEALIP/TH/NBJ/71	18.4131	0.001	15.7031	0.001	38.9411	0.004	0.8533	0.00002	1.1719	0.00002	2.1148	0.00008
SEALIP/TH/NBJ/72	18.3640	0.002	15.7010	0.002	38.8440	0.009	0.8549	0.00010	1.1697	0.00012	2.1153	0.00024
SEALIP/TH/NBJ/73	18.3070	0.002	15.6810	0.002	38.8720	0.009	0.8566	0.00010	1.1675	0.00012	2.1235	0.00024
SEALIP/TH/NBJ/74	18.3030	0.002	15.6780	0.002	38.8660	0.009	0.8567	0.00010	1.1673	0.00012	2.1234	0.00024
SEALIP/TH/NBJ/75	18.3819	0.001	15.7029	0.001	38.8595	0.003	0.8547	0.00002	1.1699	0.00002	2.1140	0.00007

Table 6 (continued)

Name	$^{206}Pb/^{204}Pb$	err (2σ)	$^{207}Pb/^{204}Pb$	err (2σ)	$^{208}Pb/^{204}Pb$	err (2σ)	$^{207}Pb/^{206}Pb$	err (2σ)	$^{206}Pb/^{207}Pb$	err (2σ)	$^{208}Pb/^{206}Pb$	err (2σ)
SEALIP/TH/NBJ/76	18.3460	0.001	15.7260	0.001	38.7718	0.003	0.8577	0.00002	1.1659	0.00002	2.1133	0.00008
SEALIP/TH/NBJ/77	18.3902	0.001	15.7188	0.001	38.8482	0.003	0.8552	0.00002	1.1693	0.00002	2.1124	0.00008
SEALIP/TH/NBJ/78	18.4039	0.001	15.6847	0.001	38.8887	0.003	0.8527	0.00002	1.1727	0.00002	2.1131	0.00008
SEALIP/TH/NBJ/79	18.3658	0.001	15.6978	0.001	38.8757	0.002	0.8552	0.00002	1.1693	0.00002	2.1166	0.00008
SEALIP/TH/NBJ/80	18.3584	0.001	15.6947	0.001	38.8739	0.004	0.8554	0.00002	1.1691	0.00002	2.1174	0.00009
SEALIP/TH/NBJ/81	18.3632	0.001	15.6961	0.001	38.8728	0.004	0.8553	0.00002	1.1692	0.00002	2.1168	0.00009

Unfortunately, such a chronological tendency, at an admittedly critical period of state formation in northeast Thai history, cannot be reliably deduced from the LI data. As Fig. 13 shows, the lead concentration of MP1 & 2 samples is, on average, substantially lower than those of MP3 & 4 samples. Hence, we may be looking at a trend from unleaded to leaded alloys - from predominantly copper LI signatures to predominantly lead LI signatures - rather than a shift in sources of copper.

Plotting the samples' LI ratios by their broad typological category is somewhat informative but the question of alloys, particularly whether leaded or not, obscures interpretative potential (Fig. 14). Likewise, plotting the NBJ samples by alloy reveals some groupings but the typological information is missing (Fig. 15). A potential solution is to combine these categories, as 'alloy-types', with typology as the first sorting criterion, being more definitively constituted, followed by alloy sub-groups (Fig. 16). Although there are some differences, it is clear the patterning thus revealed is far closer to that for typology (Fig. 14) rather than alloys (Fig. 15).

This suggests metal artefact demand by NBJ consumers was more driven by the shape of the finished product than the aesthetic or mechanical properties of the alloy. Critically, without arguing for the deliberate exclusion of one type of assemblage rather than another, this understanding would not have been achieved without our sampling of complete and recognisable funerary artefact types, rather than the typically fragmentary and unidentifiable remains from occupation contexts. Plotting by alloy-type does offer some interpretative advantage over typology alone. For example, we can distinguish a tight cluster of bronze finger rings (NBJ/79–81), which are three of a series from MP4 Burial 61. We can thus deduce that the individual likely acquired all three rings at the same time directly or indirectly from the same secondary producer, or they were placed on their hand postmortem by the individual's successors by the same supply network. The same can be said for a pair of bronze rings (NBJ/22–23) from MP2 Burial 134 and another pair (NBJ/8–9) from MP1 Burial 30. It should be noted that NBJ/7, also from Burial 30, does not plot quite so closely to its neighbours on the same finger, as although it is bronze it was recorded as a 'flat ring'. This suggests the typological distinction may have some value in discerning productions separated if not by actual workshop but perhaps by time – with different production episodes having subtle variations in feedstock.

Other consistencies include the three bronze toe rings (NBJ/24–26), also from MP2 Burial 134, indicating they were obtained as a 'lot' with the finger rings (NBJ/22–23), and bronze bracelets (NBJ/4–6) from MP1 Burial 21. This cluster is constrained to periods MP1 & 2, likewise hinting at a chronological component to the sourcing of the constituent raw materials. Of the three bronze belts, two (NBJ/56–57) plot closely and come from MP3 Burial 82,

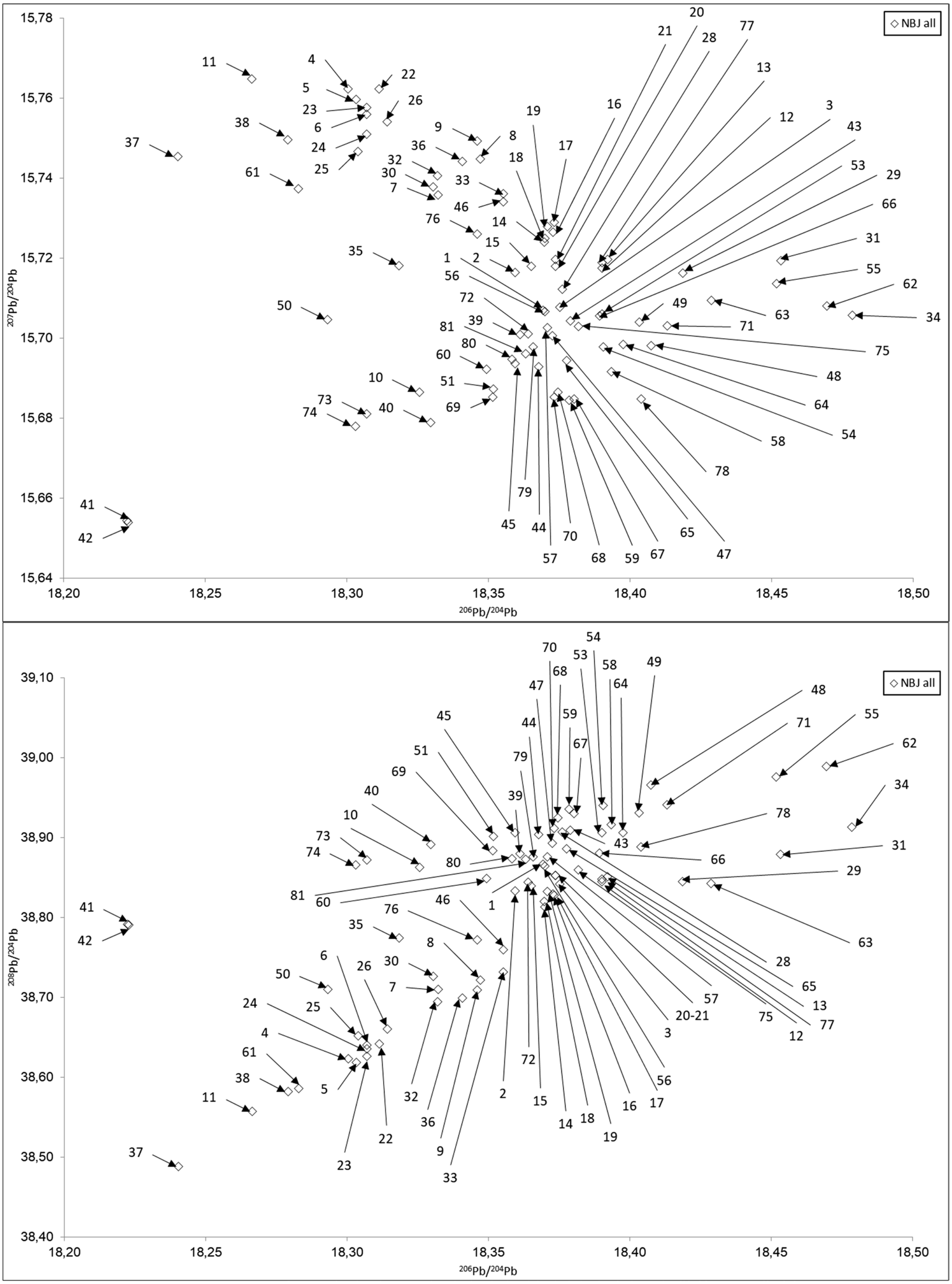

Fig. 11 Raw lead isotope ratio values for all NBJ artefacts, labelled by sample number

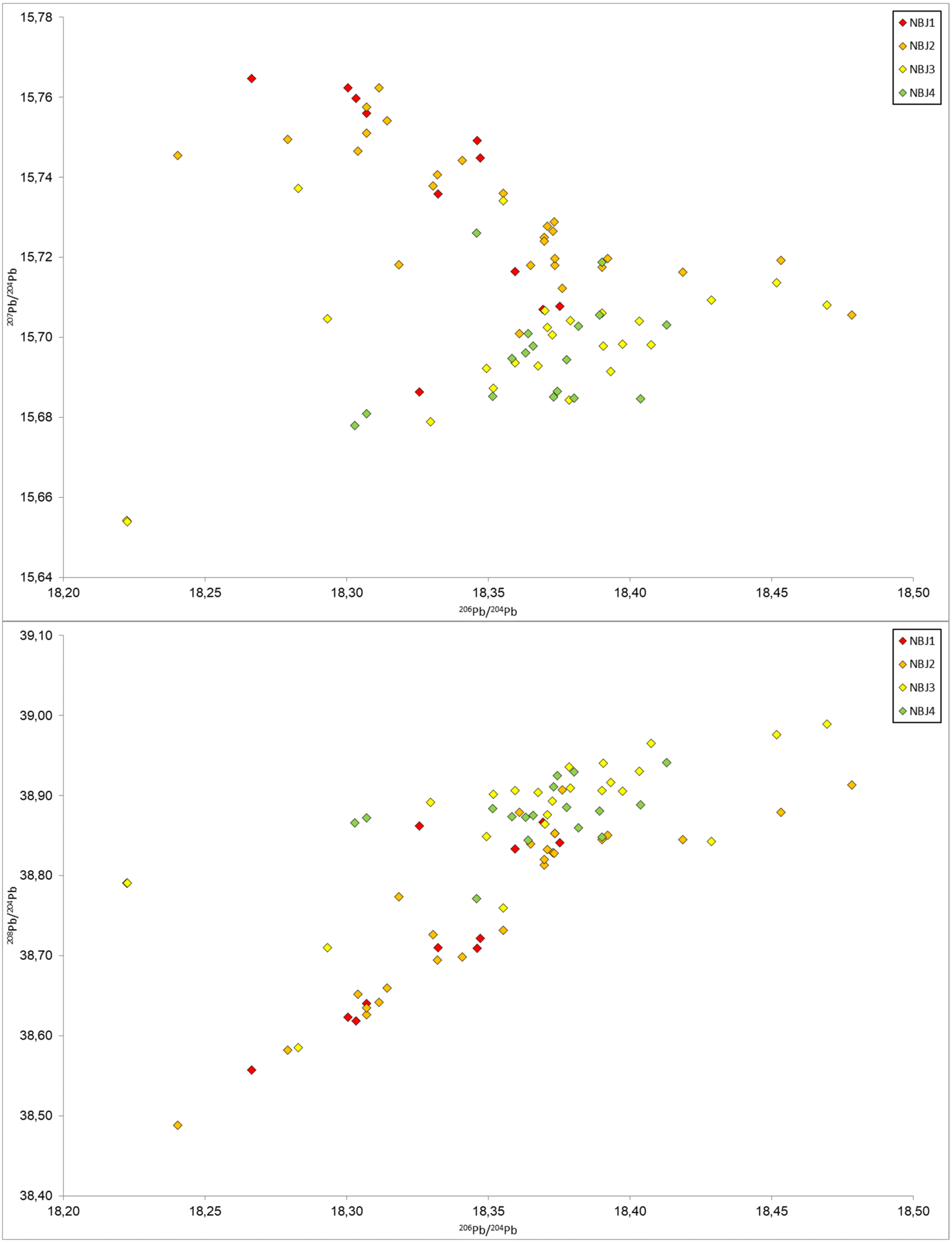

Fig. 12 Raw lead isotope ratio values for all NBJ artefacts, labelled by mortuary phase

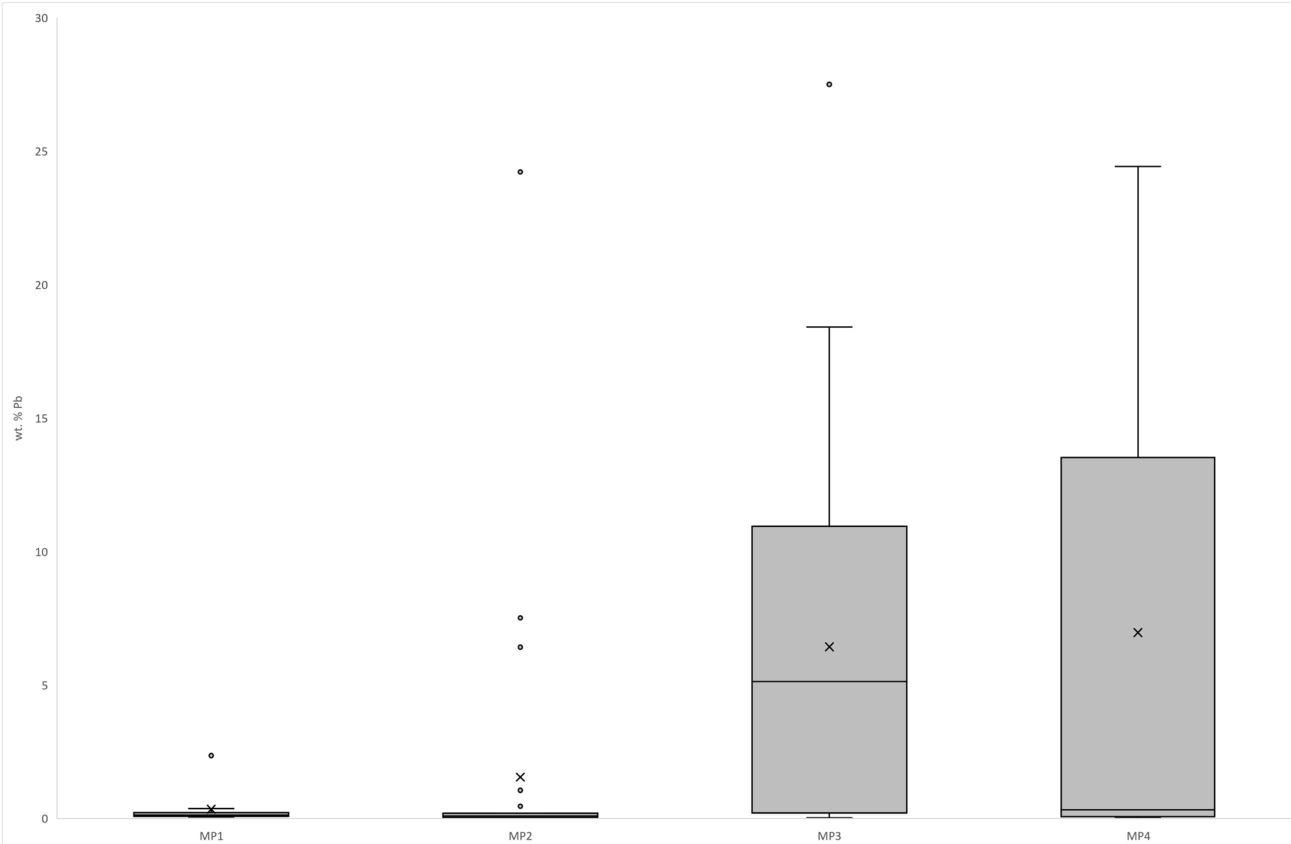

Fig. 13 Box and whisker plot for lead concentration of NBJ samples, sorted by mortuary phase

while the third (NBJ/78) comes from MP4 Burial 32. However, one must also avoid an excessive focus on numbers, as the three bronze anklets (NBJ/43–45) have over 1% uranogenic variation but are still all from MP3 Burial 46 and, in the grand scheme of things, probably still represent a single acquisition episode.

Overall, the alloy-type plot gives an impression of consistency in metal supply, both by individual burials and groups of related artefacts, and also by phase. These findings correspond well with our initial interrogation of the NBJ LI dataset, by manually assigning clusters to artefacts with triply-consistent LI ratios (Fig. 17).

The following clusters are arranged in order of uranogenic variation, based upon the first member of each group but also represent actinium series and thorogenic variation. The groups could probably be consolidated in places but we pursue the data interrogation as is, with notes on the nature and quality of the apparent consistency.

Cluster 1: NBJ/41–42, leaded bronze toe rings from MP3 Burial 46. A solid group of alloy-type and context.

Cluster 2: NBJ/38 & 61, MP2 leaded bronze bell from Burial 192 and MP3 silver copper bracelet from Burial 120. A less reliable group, mixed alloys and types. Silver could be lead-derived.

Cluster 3: NBJ/4–6, 22–26, bronze bracelets, finger and toe rings from MP1 Burial 21 and MP2 Burial 134. A reliable group of alloy and context characteristics. These two burials are located 25 metres apart on the western mound.

Cluster 4: NBJ/74–75, leaded bronze rings from MP4 Burial 7. A solid group of alloy-type and context.

Cluster 5: NBJ/10 & 40, leaded bronze flat bracelet and toe ring from MP1 Burial 35, an old adult female, and MP3 Burial 46, an adult. These burials were separated by time, but were only two metres apart. A reliable alloy group with typological difference and chronological variation, and we note that NBJ/40 was on the same finger as NBJ/41–42 (Cluster 1), showing that some artefacts were accrued from different sources/markets, potentially over time.

Cluster 6: NBJ/7, 30 & 32, bronze flat ring and two ‘bimetallic rings’ from MP1 Burial 30 and MP2 Burial 167, both infants buried 200 metres apart. A reliable alloy group with some chronological variation and sub-group contextual and typological consistency.

Cluster 7: NBJ/8–9 & 36, bronze rings and bimetallic ring from MP1 Burial 30 and MP2 Burial 167 A reliable

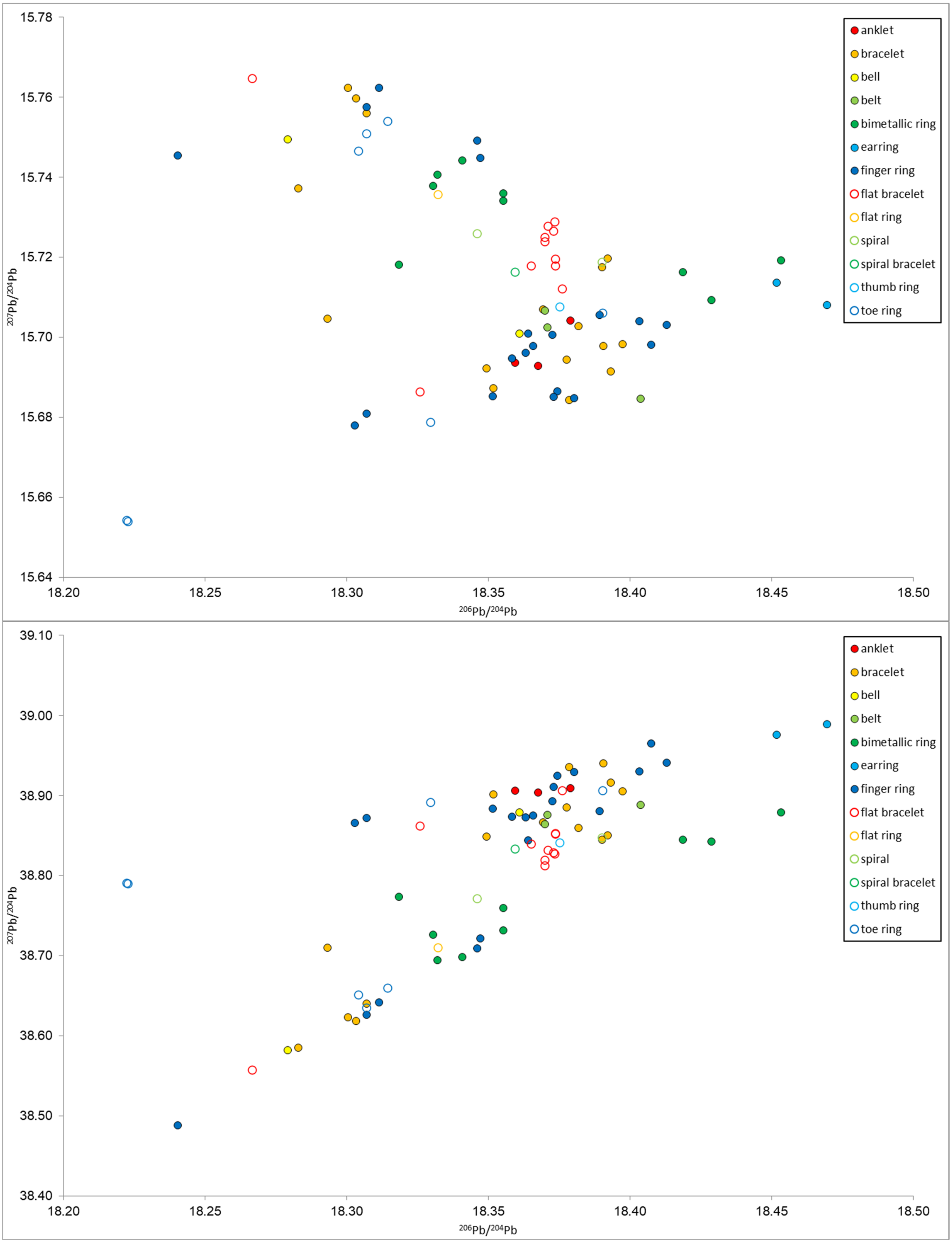

Fig. 14 Raw LI ratios for NBJ samples, plotted by typology

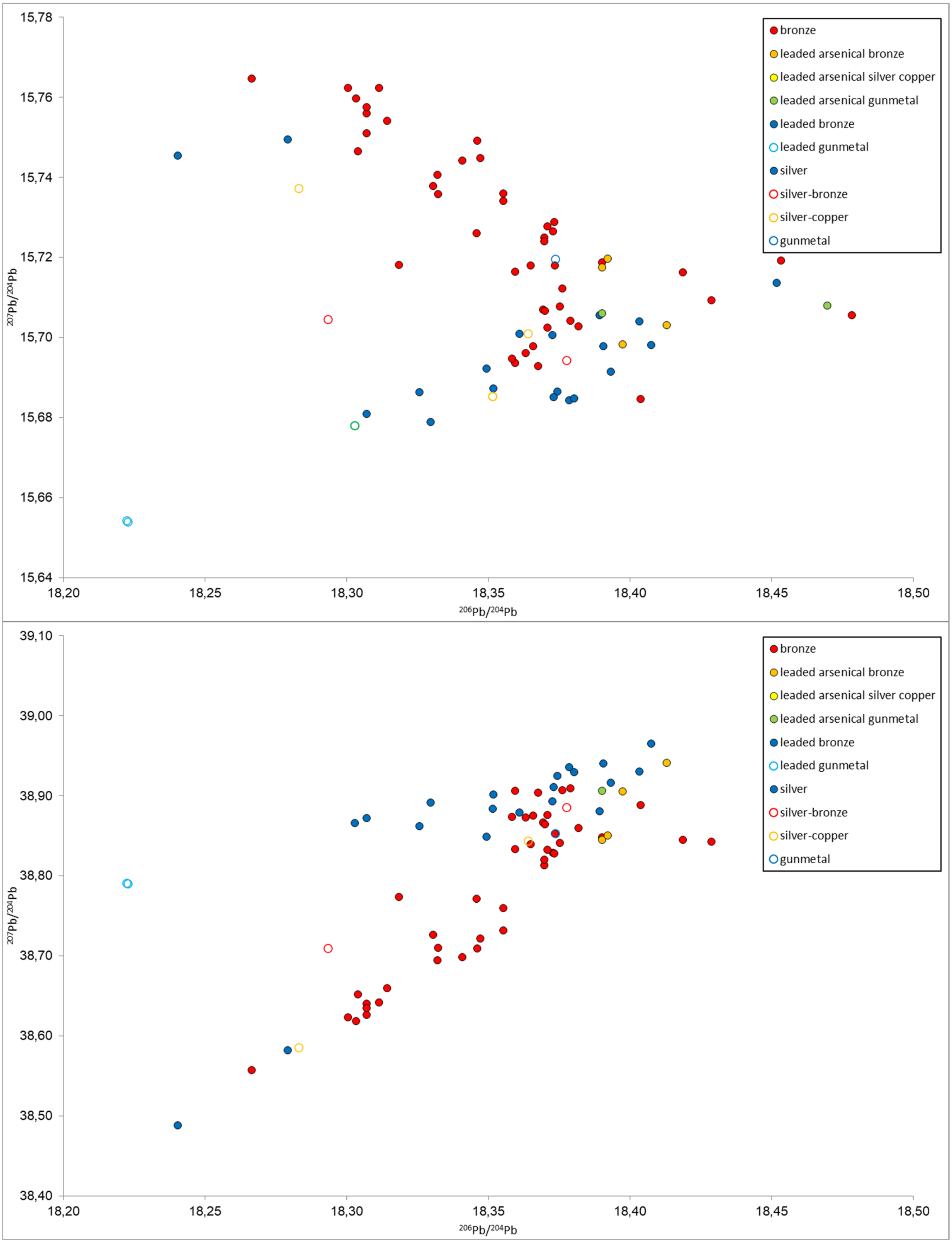

Fig. 15 Raw LI ratios for NBJ samples, plotted by alloy

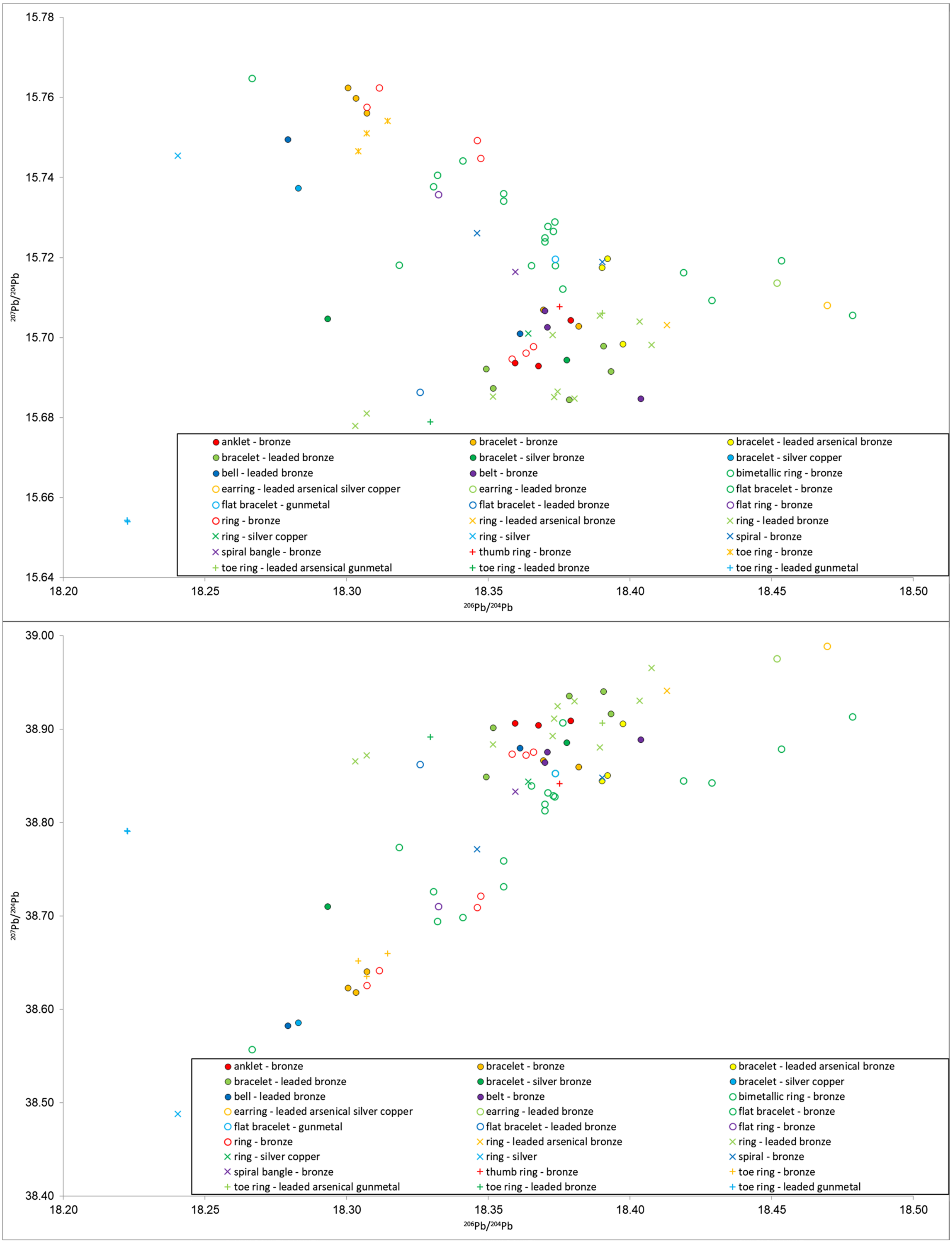

Fig. 16 Raw LI ratios for NBJ samples, plotted by 'alloy-type'

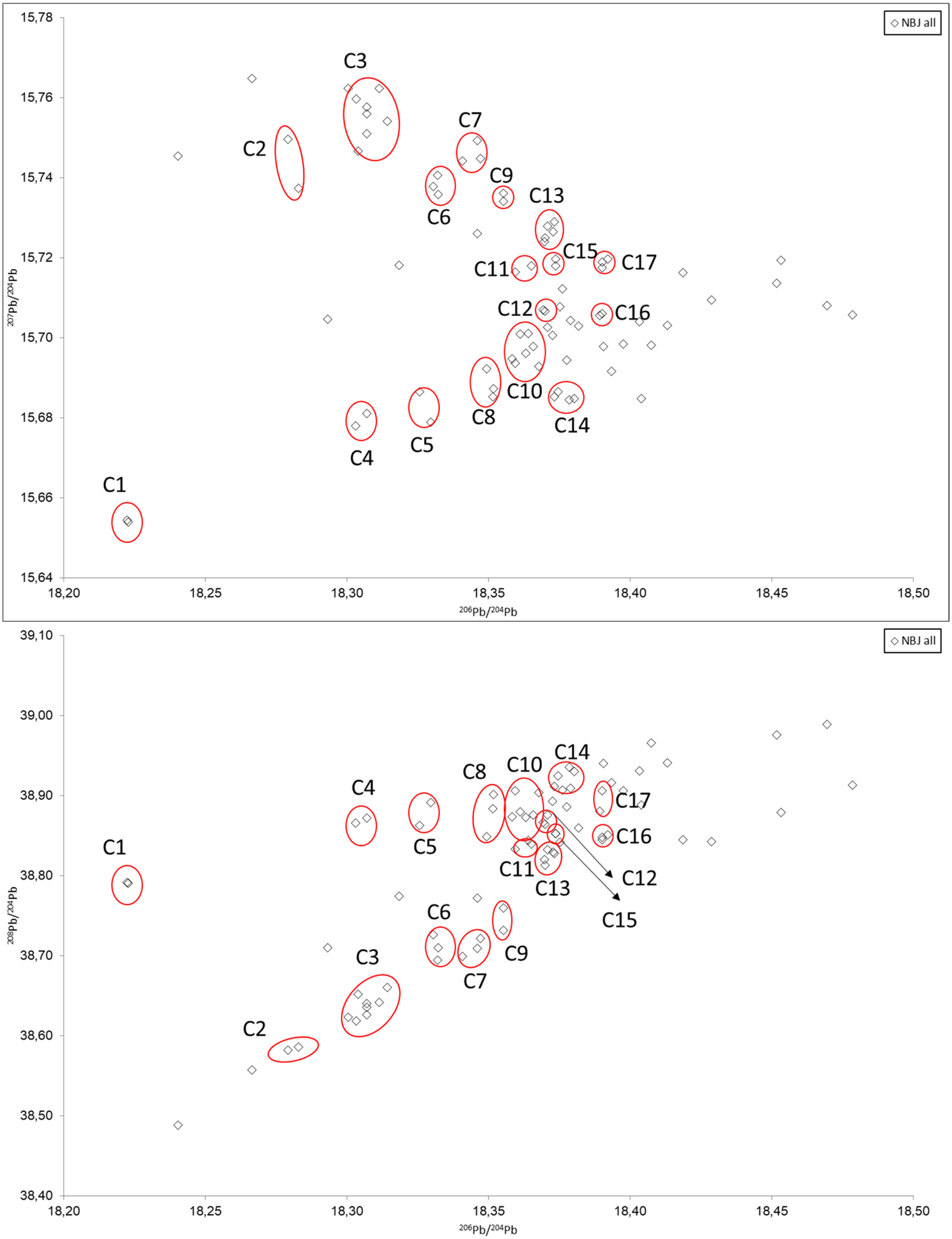

Fig. 17 Raw LI ratios for NBJ samples, marked with subjectively applied clusters of consistency across both graphs

alloy group with some chronological variation and subgroup contextual and typological consistency. We note the NBJ/8–9 rings are from the same finger as NBJ/7 in Cluster 6, and that NBJ/36 bimetallic ring is from the same finger as NBJ/30–32 in Cluster 6. This suggests either the accrual of artefacts from different sources/over time, or that Clusters 6 & 7 should be combined.

Cluster 8: NBJ/51, 60 & 69, leaded bronze bracelets and a ring from MP3 Burial 71 a mid adult female, Burial 120, mid adult male and MP4 Burial 66, and infant. A reliable alloy group with some chronological variation and chronological consistency. A shared source of lead persisting over time and across multiple individuals interred in proximity to each other.

Cluster 9: NBJ/33 & 46, bronze bimetallic rings from MP2 Burial 177, an infant and MP3 Burial 49, a young male. A reliable alloy-type group with some contextual and chronological variation. A shared source of copper persisting over time and shared by burials located ca. 200 metres apart.

Cluster 10: NBJ/ 39, 44–45, 79, 80–81, bronze bell, anklets and rings and a silver-bronze ring (NBJ/72) from MP1 Burial 61, a female, MP2 Burial 167, MP3 Burial 46 and MP4 Burial 110, a young man . A reliable alloy group present in all four mortuary phases. We note that NBJ/44–45 do not plot with NBJ/43, similarly a bronze anklet from the same burial, suggesting accrual of artefacts from different sources/over time for the same individual.

Cluster 11: NBJ2 & 15, bronze spiral and flat bracelets from MP1 Burial 18 and MP2 Burial 90, both infants. A somewhat reliable alloy group with some typological and chronological variation, which could nevertheless potentially be combined with Cluster 10.

Cluster 12: NBJ/1 & 56, bronze bracelet and belt from infant MP1 Burial 18 and MP3 Burial 82, an old male. A somewhat reliable alloy group with some typological and chronological variation, which could nevertheless potentially be combined with Cluster 10.

Cluster 13: NBJ/14, 16–19, bronze flat bracelets from MP2 Burial 90. A reliable alloy-type and chrono-contextual group, with similar artefact NBJ/15 from Cluster 11 only marginally different.

Cluster 14: NBJ/59, 67–68 & 70, leaded bronze bracelet and rings from MP3 Burial 114, aged about 15–18 years and MP4 Burials 45, an old male and 66, a three-year old. A reliable alloy group with some typological and chronological variation. We note NBJ/69, from the same individual as NBJ/68 & 80 is the same alloy-type but in Cluster 8, suggesting artefact accrual from multiple sources/over time.

Cluster 15: NBJ/20–21, bronze flat bracelets from MP2 Burial 91, an infant. A somewhat reliable alloy-type and chrono-contextual group from the same individual but could potentially be combined with Cluster 13, from the neighbouring burial of the same phase.

Cluster 16: NBJ/53 & 66, leaded bronze toe and finger ring from MP3 Burial 45, an old male, and 73 a child of about 3 months. A reliable alloy-type and chronological group, suggesting a shared lead source for artefacts for multiple individuals.

Cluster 17: NBJ/12 & 13, leaded bronze bracelets from MP2 Burial 86, an 8-month old infant. A reliable alloy-type and chrono-contextual group from the same individual.

Discussion

Intra-site

Clearly, our study of the NBJ metals assemblage is primarily funerary in nature and cannot directly be used to interpret use of metals and metallurgy in everyday life. That said, our sampling does largely reflect the settlement:cemetery distribution of NBJ metal finds, with apparently little loss or discard of metals around the homes and workspaces. Furthermore, while we have been able to identify whether assemblages of typologically similar artefacts on the limbs or appendages of deceased individuals were acquired from the same producer or intermediary, we have not studied every single artefact from every group, as our Japanese colleagues have sometimes done (Hirao and Ro 2013). This is a reflection of curatorial considerations, as LIA is always at least micro-destructive and permission will not be given (nor should it really be sought) for 100% sampling; and the perennial issue of cost, which for LIA is considerable. Nevertheless, we consider that our results demonstrate strong tendencies in NBJ funerary non-ferrous metal consumption behaviour, with individuals frequently interred with groups of anklets, bracelets or rings that were obtained from single (human, not geological) sources. When comparing the mortuary contexts for the different clusters of copper-base artefacts, we find that adult men, women and infants shared ornaments from the same potential source, and that these same sources were found in different mortuary phases. There appears to have been no restriction between the source of an ornament and the mortuary phase, age or sex of the individual wearing it.

We will deal with silver alloys below but at NBJ there was a strong trend from consuming unleaded alloys in MP 1 and 2, to leaded alloys in MP 3 and 4. For the most part we suspect that our alloy groups are not historically accurate, in that the elemental data are distorted by extreme post-depositional alteration, but our alloy-type groups convincingly indicate there were workshops producing batches of typologically similar artefacts from the same feedstock. This may have been just a few workshops, with their raw metal supply varying over time, or many foundries using a multitude of primary metal suppliers and/or metal recycling pools.

Resolving this question satisfactorily will require the full technological and geochemical analysis of secondary production workshops from a wide range of places and periods. While NBJ did not have any evidence for foundry activity, this high-density sampling of a long-lived site is nonetheless a significant step forward for understanding diachronic trends in Iron Age MSEA metal supply, which is our next stop.

Primary production

Only three prehistoric copper producing loci are currently known and technologically and geochemically studied in MSEA: the Khao Wong Prachan Valley (KWPV) in central Thailand (Pryce et al. 2010, 2011a, 2024; Cadet et al. 2024), Phu Lon (PL) in northern Thailand (Pryce et al. 2011b), and the Vilabouly Complex (VC) in central Laos (Pryce et al. 2014; Cadet et al. 2019, 2022). A lead producing locus, Song Toh (ST) in west-central Thailand, is also known and geochemically characterised (Hirao and Ro 2013) but the chronology and technology are unstudied. Of these loci, the KWPV is by far the closest, at ca. 165 km geodesic west, followed by PL at 325 km north, ST at 350 km west, and VC at 450 km geodesic northeast. You would therefore be forgiven for assuming that the KWPV primary copper production site cluster, which includes Khao Sai On, Nil Kham Haeng, Non Pa Wai, Phromatin Tai and Tha Kae, was the mostly likely candidate for NBJ copper-base consumption. This assumption would be grievously erroneous (Fig. 18), as not one of the 79 NBJ samples, of which 51 are unleaded, is even remotely consistent with the KWPV, nor with PL. This outcome is not surprising as the lack of distribution for central Thai copper has been noted for many years (Pryce et al. 2014, 2017b, 2023), and has recently been confirmed *within the producing region itself* (Pryce et al. 2024) – copper smelters at Khao Sai On, Phromatin Tai and Tha Kae all imported copper/bronze from the VC or a primary producer with a very similar signature. This might have been a chronological issue, as while the main KWPV sites of Non Pa Wai and Nil Kham Haeng were certainly active in the Bronze Age (Higham et al. 2020b), it is uncertain they were producing copper in the Iron Age. However, recent analyses demonstrate that Khao Sai On, Phromatin Tai and Tha Kae all have production phases contemporaneous with NBJ (Cadet et al. 2024), so it is apparent that NBJ consumers did not get their metal from the nearest available source. There is consistency between some NBJ leaded artefacts and the ST signature in west-central Thailand, which is interesting as the lead metal or leaded alloys so sourced would have likely transited the copper producing region of central Thailand in order to reach northeast Thailand. Of course, were west-central Thai lead to be alloyed with central Thai copper, the LI signature of the latter would be completely overwhelmed by the former but in the recent KWPV area case study, it was interpreted as unlikely that this was occurring (Pryce et al. 2024). In any event, it is clear there were other lead producing communities of whom we have as yet no trace.

However, while it would initially appear that NBJ unleaded metal is consistent with copper production at the VC, closer examination suggests that the hegemony of VC copper supply does not give the full picture for NBJ (Fig. 19). Archaeometallurgical research by Cadet et al. (2019, 2021, 2022) has demonstrated that the VC copper ingot typologies have subtly varying LI signatures, doubtless related to the differential exploitation of closely-related copper mineralisations in the locality. Importantly, the bowtie ingots are stratigraphically the oldest, potentially Bronze Age, whereas the conical ingots are certainly Iron Age, and the bowl ingots are uncertain having been found by UXO teams. When we examine the LI data clouds, we see the bowtie ingots are highly consistent with each other, and inconsistent with NBJ consumption. Conversely, there is some consistency between some of the NBJ unleaded artefacts and the conical and bowl ingots, which would make sense due to Iron Age contemporaneity. That does leave, however, a considerable proportion of the NBJ unleaded copper-base assemblage that is not closely compatible with the VC signature but for which the general consistency implies there are further unknown copper producers in the area. This is a perfectly reasonable outcome, and was always accounted for within the SEALIP/BROGLASEA methodology (Pryce et al. 2011b, 2014), in that increasing LI data density would lead to multiple interpretative revisions as resolution increased our capacity to discern new patterns.

We now turn to the issue of 'bimetallic' artefacts, so called as they were thought by the excavators, at NBJ and other regional sites, to be made of iron or an iron-copper alloy due to their mass and reddish corrosion products. As addressed above in elemental results, these artefacts are not made of iron but in their latter suggestion the excavators are partially correct, in that they have elevated iron contents. However, this is not due to the deliberate alloying of iron and copper, which would be impossible as iron has too high a melting temperature to be made liquid in protohistoric MSEA. Rather it is due to either the smelting of copper from ferruginous ore or fluxed with iron oxide in excessively reducing conditions, or because of the post-depositional environment, or a combination of the two. Intriguingly, 'bimetallic' ingots were noted by the excavators at the Vilabouly Complex, again assumed to be iron but actually copper (Cadet et al. 2019). Therefore, we checked the LI consistency of NBJ bimetallic rings and the VC bimetallic ingots, which showed some but by no means outstanding correspondence. Nevertheless, we consider it highly inadvisable

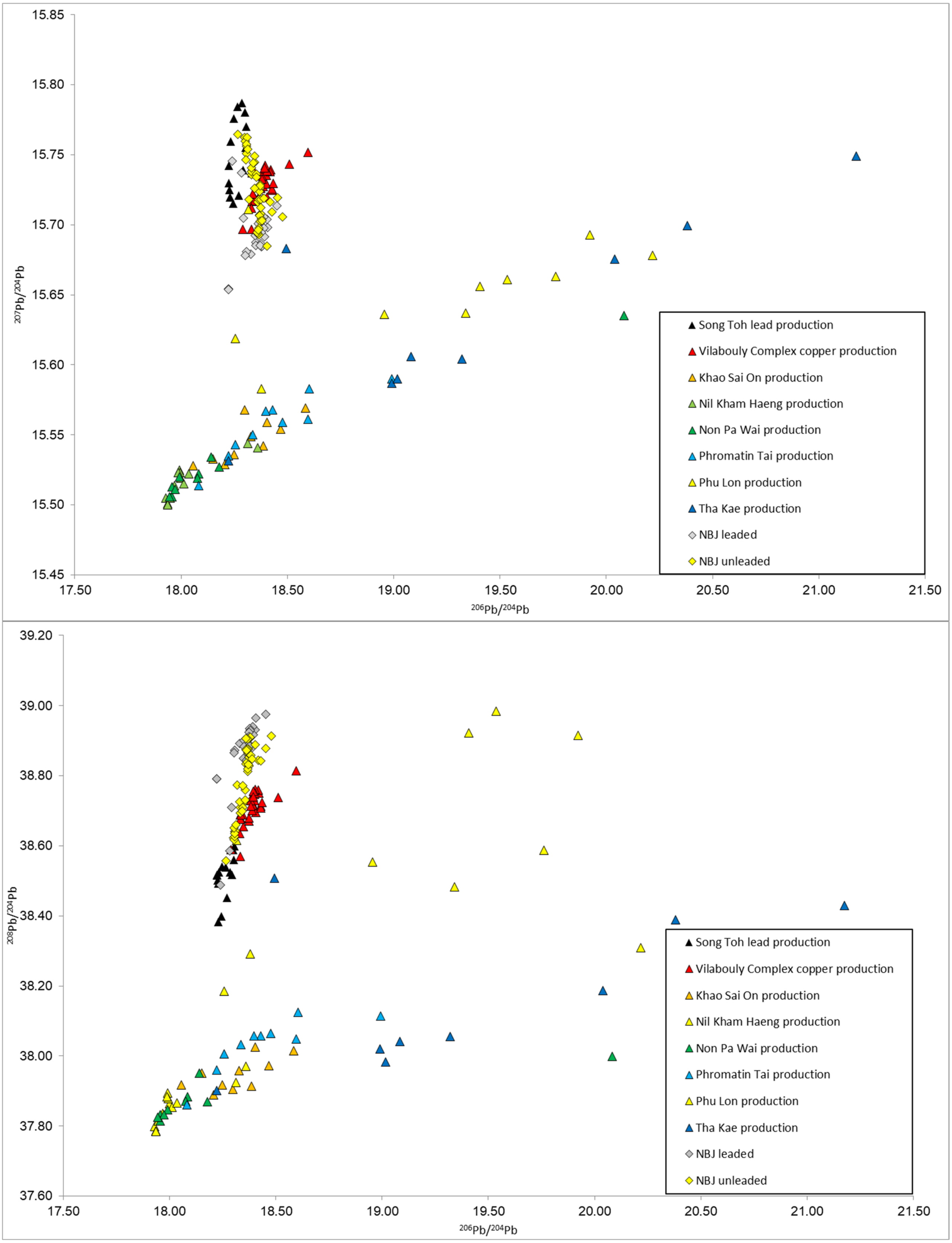

Fig. 18 Raw LI ratio data for NBJ leaded and unleaded artefacts, plotted against MSEA primary copper and lead production signatures

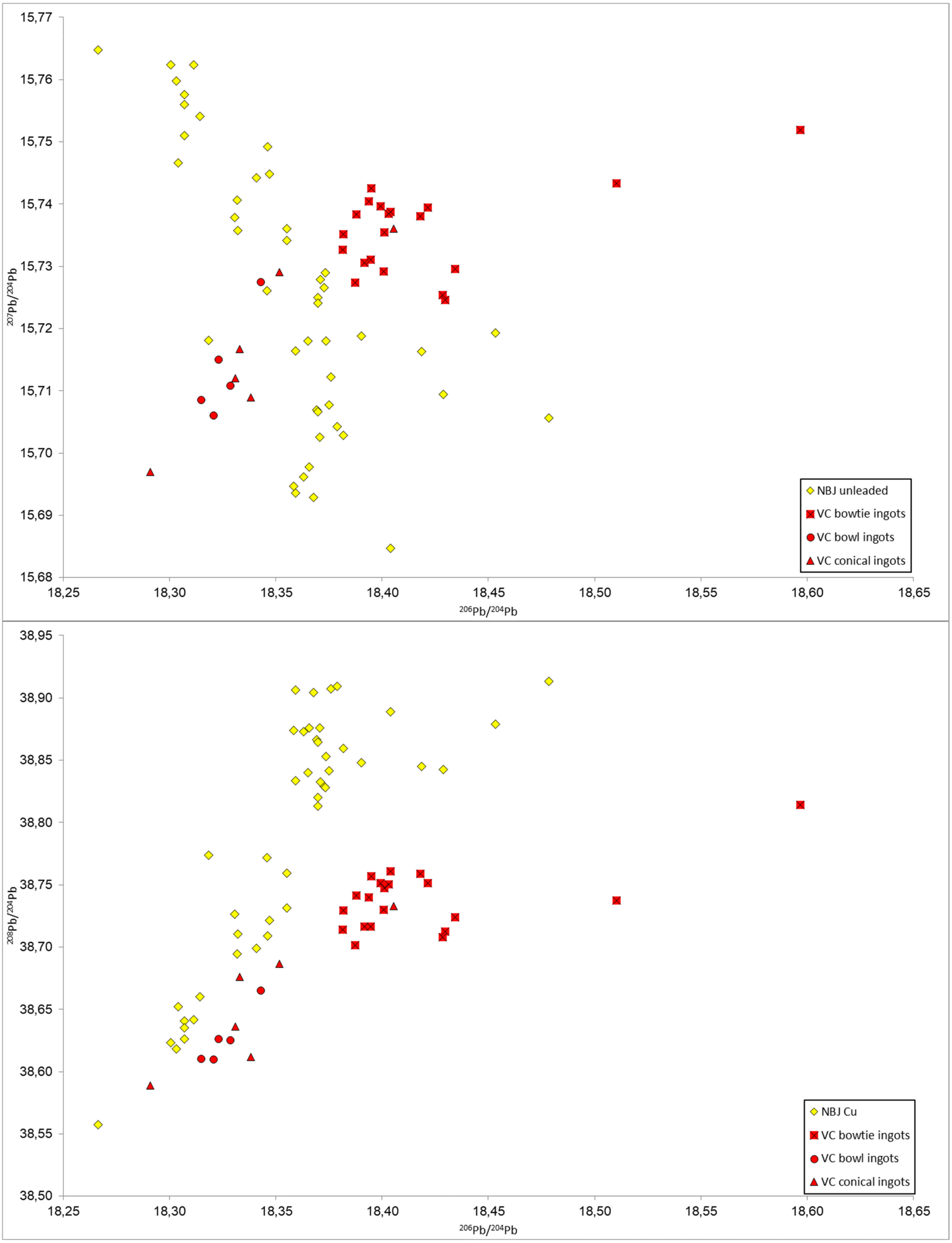

Fig. 19 Raw LI ratios for NBJ unleaded artefacts plotted against VC copper ingot typologies

to assume unanalysed 'rusty' objects are iron as opposed to unrefined copper/bronze, which may indeed be the case for BNW artefact cat. 617 in Bronze Age 4 Burial 34 (White and Hamilton 2018: 87).

Secondary production and consumption

We lack comprehensive studies of secondary production workshops, which might identify consistent signatures in metallurgical paraphernalia, e.g., crucibles and moulds, consistent with finished artefacts from consumption sites. Therefore, we are obliged to jump to the stage of comparing Iron Age copper-base and leaded copper-base consumption assemblages, which we will do in order of proximity.

Northeast Thailand

NBJ is part of a site cluster in the Upper Mun River Valley: BLK, BNW, NUL and NMK, investigated over three decades by the Origins of Angkor Project (Fig. 2). Regrettably, BLK, NUL and NMK were all excavated prior to SEALIP/BROGLASEA's initiation in 2008 (Higham and Thosarat 2004; Higham et al. 2007), and thus their assemblages were not incorporated in the regional study. However, 20 BNW samples, 10 each from Bronze and Iron Age contexts, were sampled in 2009 (Pryce 2011; Pryce et al. 2014) and a single NUL unleaded bronze ornament (Cat. #504) from Mortuary Phase 4 infant Burial 25 in Cluster B (Higham et al. 2007: 193). Also in northeast Thailand, but located around 250 km north in the Chi River catchment, Iron Age samples from Ban Chiang (SEALIP/TH/BC/13–17) and Don Klang (SEALIP/TH/DK/1–3) were sampled in 2009 (Pryce et al. 2014; Pryce 2019).

The sole NUL bronze sample is broadly consistent, as might be expected given the site's proximity, but without any standout associations (Fig. 20). From also neighbouring BNW, three Iron Age 1 (420-200 BC) samples (BNW/11–13), a lead fragment and two leaded bronze 'cordiforms' (a shape recognisable in the KWPV as copper ingots but here not the case as they are leaded alloys) from Burials 417 and 482 are consistent with NBJ/37, the MP2 (AD 400–550) silver ring. This suggests the latter's silver may have been cupellated from an argentiferous lead source also exploited for lead metal up to eight centuries earlier (BNW/11 has 0.5 wt. % Ag). Furthermore, BNW/19, an Iron Age 3 (AD 200–400) bronze spiral ornament from Burial 111 has good consistency with NBJ Cluster 3, Iron Age 3 leaded bronze (BNW/17) and bronze (BNW/18) bracelets from Burial 101 have general consistency with NBJ Clusters 10–11, BNW/15 & 20, an IA1 leaded bronze bracelet from Burial 232 and an IA4 (AD 300–500) bronze vessel are broadly consistent with NBJ Clusters 6 & 7 and BNW/16, an IA2 (200 BC - AD 200) bronze bracelet from Burial 266 plots in the cloud of dispersed NBJ samples more uranogenic than Cluster 17. In all these cases the BNW samples plot within the NBJ data clouds, and in the specific cases of cluster consistency it is possible they were acquired from the same producer or intermediary at both sites.

Moving further afield, BC offers far less compatibility, probably due to the much greater distance and thus dissimilar transportation and metal networks. BC/15, a late Iron Age bronze wire, shows consistency with NBJ Clusters 4 and possibly 5, but these are leaded bronzes and thus the association may be coincidental. DK/2 & 3, late Iron Age and late Iron Age/Early Historic bronze bracelets, respectively, have reasonable but not specific consistency with NBJ bronzes, while DK/1, another late Iron Age bronze bracelet, has even less compatibility but still more than most BC samples.

Central Thailand

We have already established the lack of NBJ compatibility with central Thai copper production signatures, and this extends to a number of the consumption signatures: Ban Mai Chaimongkol, KSO and PTT (Fig. 21). Ban Pong Manao (BPM) presents two interesting patterns, firstly in the broad consistency of BPM leaded artefact signatures with those from NBJ, and secondly in the near total incompatibility of BPM unleaded artefacts with those from NBJ. Two exceptions, bronze bracelets BP1805 and BP1807, exhibit reasonable consistency with NBJ Clusters 6 & 7 but generally we can say that BPM and NBJ have dissimilar supply networks for copper but potentially overlapping supply networks for lead. The Ban Khu Muang samples are all leaded and, like some of the BPM leaded samples, are highly consistent with NBJ Cluster 2. The single leaded copper sample from Ban Pong Takhob is broadly compatible with NBJ leaded alloys but not to any specific cluster. The sole unleaded alloy from Sab Champa, a bronze axe, has no compatibility with NBJ unleaded samples but SCP/2, a leaded bronze bracelet has general consistency with NBJ leaded samples, and SCP/3, a leaded bronze animal figurine, is highly consistent with NBJ Cluster 2. Overall, the central Thai comparators suggest that while NBJ shared little to no copper/bronze sources, they did share lead sources. As these sources, particularly Cluster 2, may be in west-central Thailand, it implies that that lead exchange network traversed central Thailand without participating in local copper exchange markets.

NW Cambodia

The two Lovea leaded samples have internally variant values but are broadly consistent with the NBJ leaded alloy range of LI ratio values (Fig. 22). Conversely, the Lovea unleaded samples are internally highly consistent and are also compatible with NBJ Clusters 10–13. Of the Prei Khmeng leaded

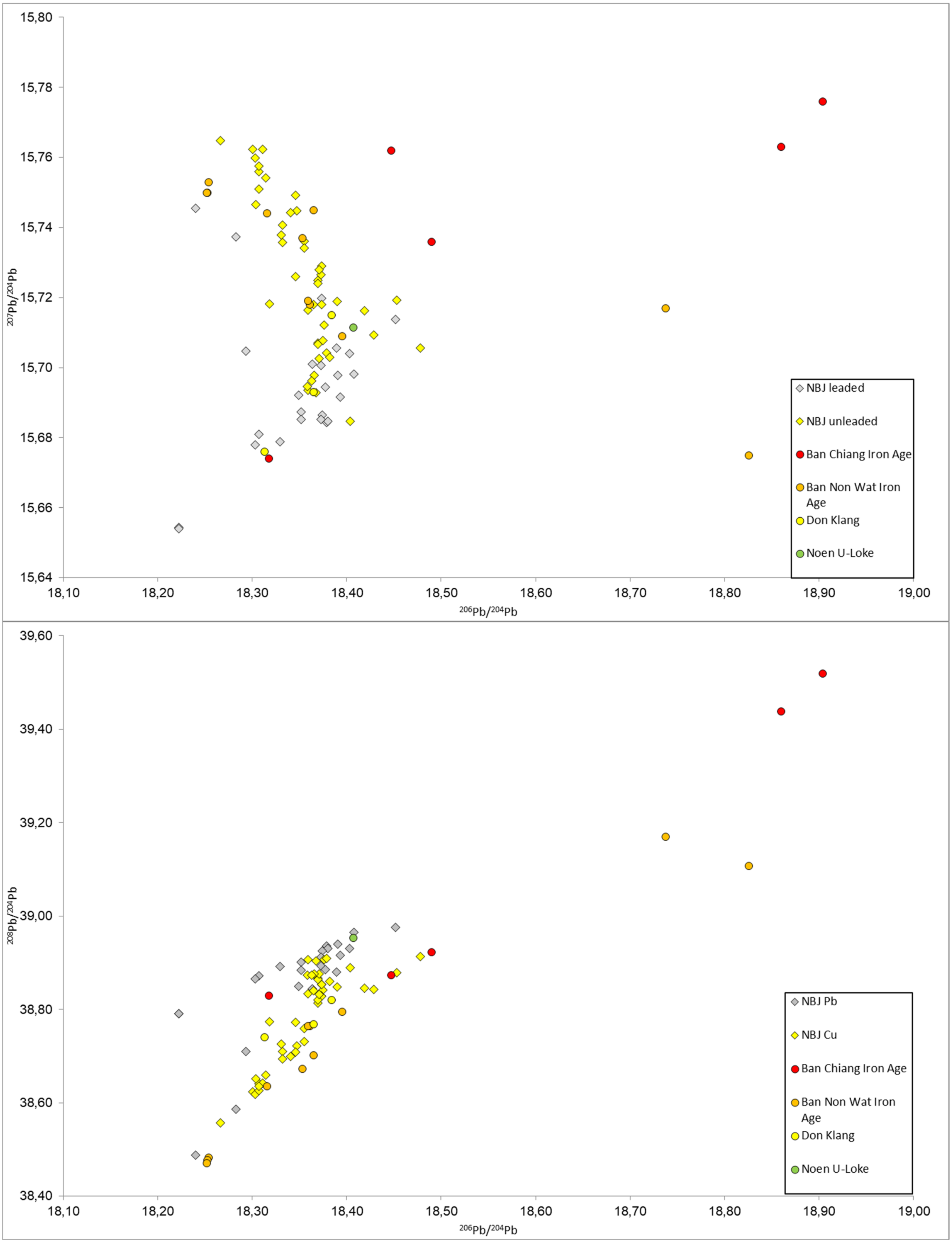

Fig. 20 Raw LI ratio data for NBJ samples plotted against those for northeast Thai sites (Pryce et al. 2014; Pryce 2019)

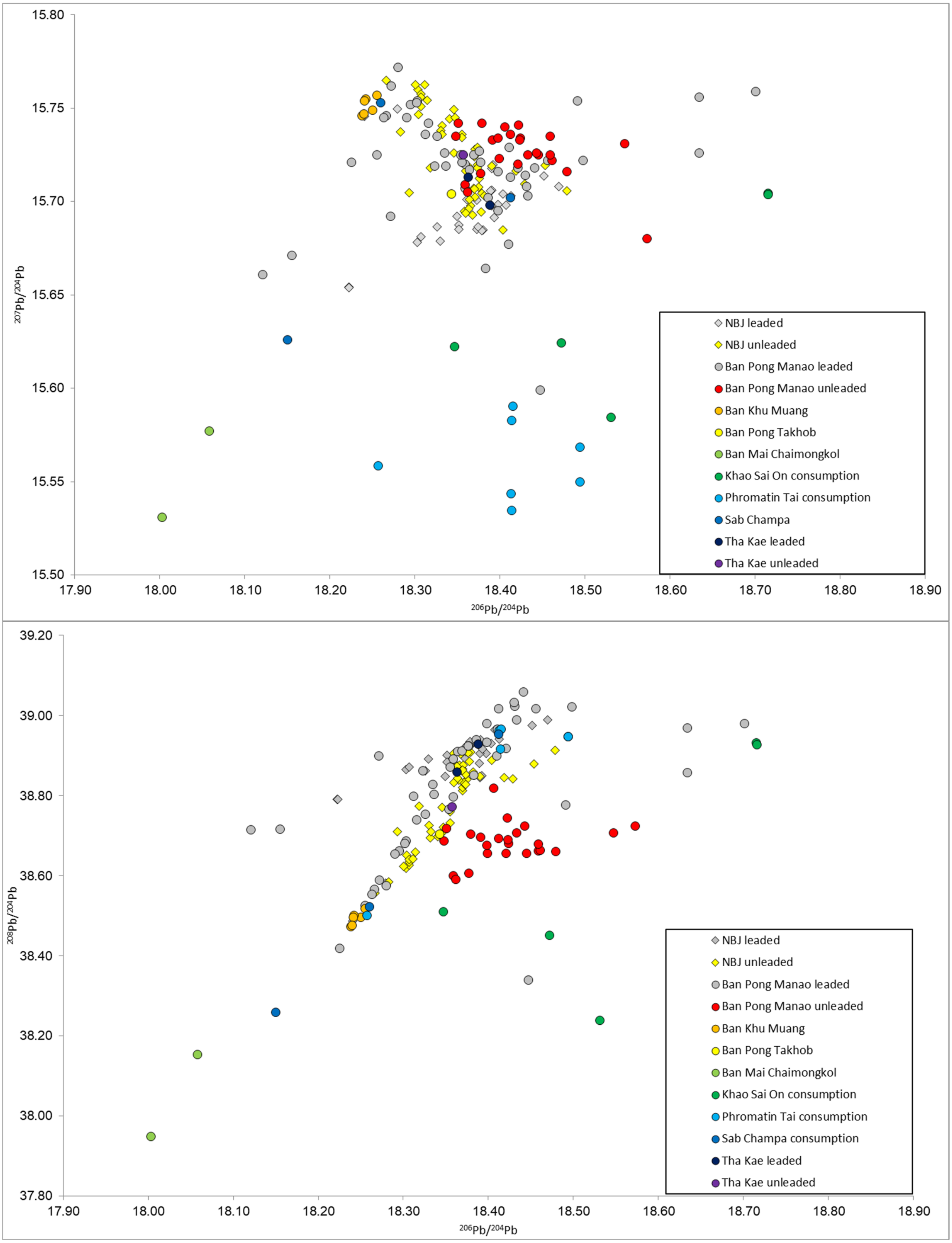

Fig. 21 Raw LI ratio data for NBJ samples, plotted against central Thai sites with at least some consistency (Hirao and Ro 2013; Pryce et al. 2024)

bronzes, fragment PKM/8 is highly radiogenic and plots off the scale, PKM/2, a lead strip, has reasonable consistency with NBJ leaded artefacts, but PKM/10, a leaded bronze bracelet, is consistent with Cluster 8. Like Lovea, the Prei Khmeng unleaded artefacts are internally consistent and likewise compatible with Clusters 10–13. The relatively few Phum Snay leaded artefacts have good compatibility with NBJ leaded Clusters 14, 16 & 17 but it is with Phum Snay's unleaded artefacts that we observe particularly interesting patterning. The granularity of Phum Snay's LI data (Hirao and Ro 2013) has previously been noted and re-interpreted to potentially represent offerings within specific burials (Pryce et al. 2017b). Plotted against NBJ unleaded samples there is a general consistency but also two instances of high compatibility: firstly with Clusters 10 & 11, and secondly with Cluster 3.

We find the latter more intriguing, as Cluster 3 is better distinguished than the others and represents NBJ MP1 & 2 middle-aged and elderly male Burials 21 & 134. The Phum Snay bronze samples plotting in and around Cluster 3 were from Burial 6 in the upper levels of Location L of the 2010 Japanese excavation, dating to around the 1st c. AD (Hirao and Ro 2013: Table 8.15). There is some difficulty cross-referencing with the Phum Snay funerary data (Matsushita and Matsushita 2013) but it appears Burial 6 was a male of 156–161 cm height, interred in a flexed supine position with his head to the east. He is described as "mesokran", with a "short and broad" facial cranium, "alveolar prognathism" and not having undergone teeth removal or sharpening like other individuals from the cemetery. We leave it to our bioarchaeologist colleagues to establish whether there is a potential connection between the burials associated with Cluster 3, however, to the best of our knowledge, this is the first time in MSEA that the grave goods of specific individuals can be archaeometrically-linked, not just in different cemeteries but different provinces and countries. This is not, of course, to say that no attributes have previously been noted between northeast Thailand and northwest Cambodia – this being the basis of the P2P project. In addition to moated sites (O'Reilly and Scott 2015; O'Reilly et al. 2017), funerary data also show shared traditions of individuals been laid upon beds of rice and with offerings of pig limbs, as well as the presence of distinct pottery types, like 'Phimai black' (Lim 2020; O'Reilly et al. 2020). Notably, as all the linked individuals are mature males, this patterning supports regional interpretations, mostly based on strontium isotope studies, for matrilocality being commonly practiced (Bentley et al. 2021).

Furthermore, a recent study of NBJ glass beads (Dussubieux et al. 2024), offers elemental and isotopic results against which we can compare elemental glass data from northwest Cambodia (Carter et al. 2023) and our metals data. Potash glass is rare at NBJ, as opposed to peninsular Thailand and Myanmar but this may be due to the earlier chronology of those sites. However, m-Na-Al1 glass is found in all NBJ phases, as it is at nearby Iron Age BNW and NUL and at Phom Lovea, Phom Sophy and Prei Khmeng in northwest Cambodia. Not only do these glass types align with our metals data in tying these sites together as part of Carter et al.'s (2023) post AD 200 "Mekong Interaction Sphere", but also links to southern India/Sri Lankan glass supply networks (Dussubieux et al. 2024); themselves several centuries later than the other South Asian glass types associated with the earliest Iron Age sites in littoral MSEA (Dussubieux and Bellina 2018).

At this juncture we would like to push the interpretative boat out – why should some of our unprovenanced metal artefact clusters not find their source in South Asia? By the time NBJ was occupied, South-Southeast Asian contact had been in operation for up to seven centuries, including the limited movement of South Asian stone specialists (Bellina 2003, 2014, 2017), with exchange of pottery (e.g. Northern Black Polished Wares, Bouvet 2017), food and/or crops (Castillo 2017) and the aforementioned glass (Dussubieux and Bellina 2017) well established. Why not then metal, especially as we see South Asian-associated metallurgy from the earliest contact periods (Pryce et al. 2017a; Pryce and Bellina 2018) and there is even limited aDNA evidence for South Asian individuals in Cambodia during the early centuries AD (Changmai et al. 2022). We certainly do not argue for partial South Asian metal supply as a certainty or truth but given the near total lack of non-ferrous archaeometallurgical research in southern India (with the exception of some Chola bronzes, Srinivasan 1999), we absolutely consider it an avenue worthy of investigation.

Conclusion

The study of 79 Non Ban Jak non-ferrous metal artefacts demonstrates beyond reasonable doubt that the nearest copper supply, from central Thailand, was not a source but that lead metal, and possibly silver, from west-central Thailand were likely exchanged through to northeast Thailand. Numerous clusters of high lead isotope ratio consistency artefacts have been noted throughout the NBJ cemetery, accounting for alloys, phases and typologies, suggesting widespread and persistent acquisition of finished copper-base artefacts from a range of, potentially secondary, producers. The Vilabouly Complex of central Laos is present as a copper supplier to NBJ but, given much greater data density and the detection of subtle variations in LI data patterning, not as the dominant source as has been thought for the last fifteen years. This rather depends on the definition of the Vilabouly Complex, as the similarity of some of the

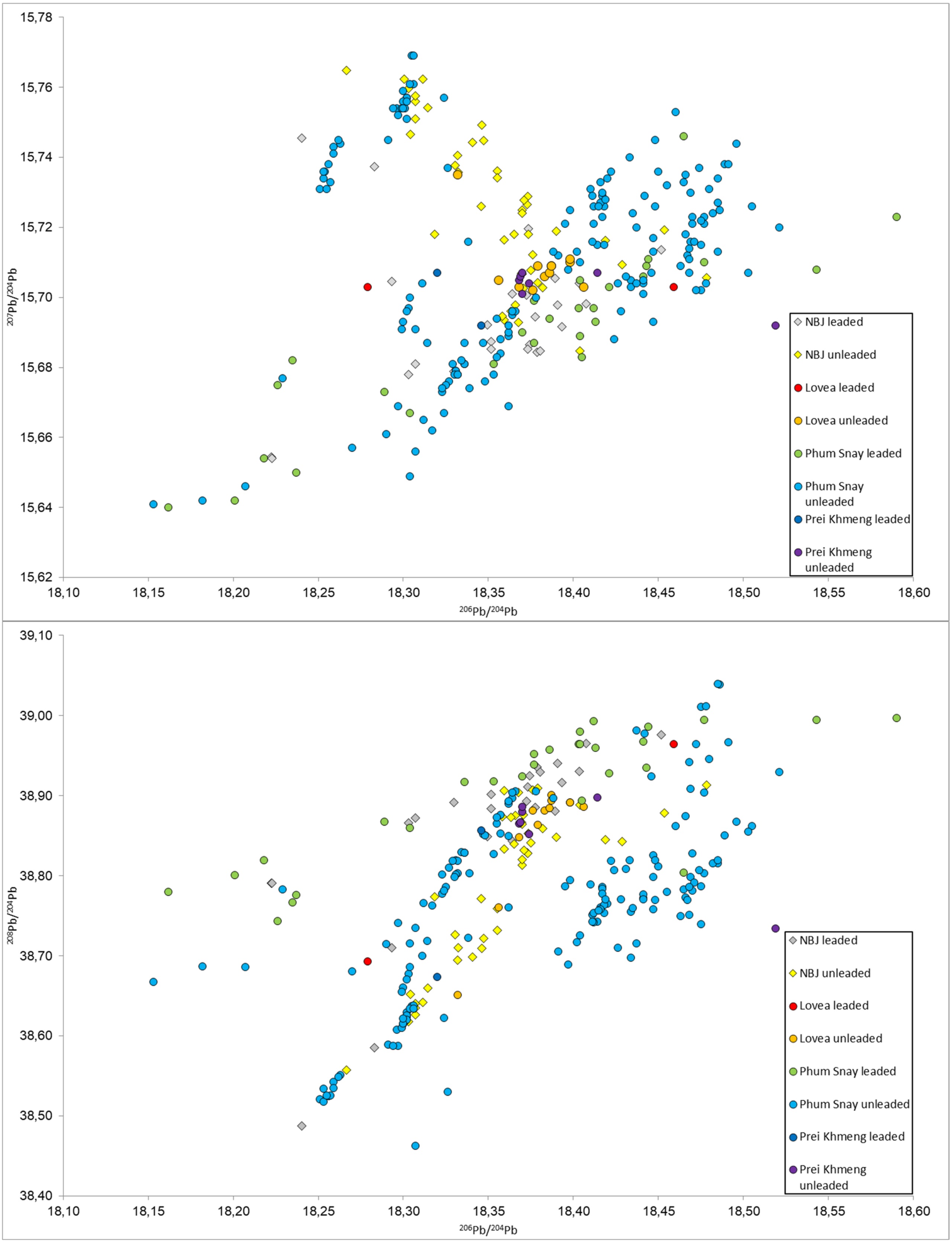

Fig. 22 Raw LI ratio data for NBJ samples plotted against those from northwest Cambodian sites (Hirao and Ro 2013; Pryce et al. 2014). Axes constrained to remove two Phum Snay and one Prei Khmeng samples whose values reduced plotting clarity for the majority

LI signatures suggests further, unknown, primary copper producers remain to be found in central Laos.

We have identified multiple consistencies with grave good copper-base metal consumption in neighbouring contemporary cemeteries at Ban Non Wat and Noen U-Loke but only weak compatibility with copper-base consumption assemblages in central Thailand. Lead-base consumption patterning, however, seems consistent across the two regions. Furthermore, we have not only established multiple links with copper-base consumption assemblages at Prei Khmeng, Phum Lovea and Phum Snay in northwest Cambodia, we have associated contemporary individual burials at Non Ban Jak and Phum Snay, which we believe is a regional material culture first. Non Ban Jak was, on pottery, glass, funerary practice and now nonferrous metals data, an active member of the 'Mekong Interaction Sphere', likely exchanging salt for exotic goods. Finally, given the number of unknown LI signatures in the NBJ assemblage, and pre-existing links to South Asia, we propose the investigation of southern Indian copper mineralisations as potential sources for *some* MSEA later Iron Age copper-base metal consumption.

Acknowledgements We particularly wish to thank Dr Thosarat Ratchanie, who was co-director of the Non Ban Jak excavation and who managed the NBJ collections in Phimai. We also thank the Thai Fine Arts Department and the Thai National Research Council of Thailand, for their kind permission to carry out excavations and post-excavation studies. We are especially grateful to Dr Enrique Vega (CNRS), who carried out the SEM-EDS analyses for this study.

The Paddy to Pura – Origins of Angkor Project was generously funded by the Australian Research Council from 2011 to 2017 (https://dataportal.arc.gov.au/NCGP/Web/Grant/Grant/DP110101997) and the excavation of Non Ban Jak was also financially supported by the Marsden fund of New Zealand. The archaeometallurgical programme, Bronze and Glass as Cultural Catalysts and Tracers in Early Southeast Asia, c. 1000 BC to c. AD 500, was supported by the French Agence National de Recherche from 2016-2021 (https://anr.fr/Projet-ANR-16-CE27-0011).

Finally, we offer our gratitude to the anonymous reviewers, who gave most welcome constructive criticism; though all faults remain our own.

Author contributions T.O.P. and C.F.W.H. wrote the main manuscript text and prepared the figures. Site excavation was co-directed by C.F.W.H. Metallurgical analyses were performed by T.O.P. with the MC-ICP-MS outsourced. All authors reviewed the manuscript.

Funding The analytical work in this paper was supported by the French Agence National de Recherche 'BROGLASEA' project. The fieldwork and dating programmes were supported by the Australian Research Council 'Paddy to Pura' project and the New Zealand Marsden Fund "Dating the prehistory of Southern China and Southeast Asia" and 'The origins of social inequality in Southeast Asia: an exploration of health and wealth disparity at the emergence of state level society' projects.

Data availability No datasets were generated or analysed during the current study.

Declarations

Competing interests The authors declare no competing interests.

References

Aebischer S, Cloquet C, Carignan J, Maurice C, Pienitz R (2015) Disruption of the geochemical metal cycle during mining: Multiple isotope studies of lake sediments from Schefferville, subarctic Québec. Chem Geol 412:167–178. https://doi.org/10.1016/j.chemgeo.2015.07.028

Bellina B (2003) Beads, social change and interaction between India and Southeast Asia. Antiquity 77:285–297

Bellina B (2014) Maritime Silk Roads' Ornament Industries: Socio-political Practices and Cultural Transfers in the South China Sea. Camb Archaeol J 24:345–377

Bellina B (ed) (2017) Khao Sam Kaeo: a late prehistoric city of the Upper Thai-Malay Peninsula. Ecole française d'Extrême-Orient, Paris

Bellina B, Favereau A, Dussubieux L (2019) Southeast Asian early Maritime Silk Road trading polities' hinterland and the sea-nomads of the Isthmus of Kra. J Anthropol Archaeol 54:102–120. https://doi.org/10.1016/j.jaa.2019.02.005

Bentley RA, Pradier B, Kyaw AA, Pryce TO (2021) Kinship and migration in prehistoric mainland Southeast Asia: An overview of isotopic evidence. Archaeol Res Asia 25:100260. https://doi.org/10.1016/j.ara.2021.100260

Bernard, M.C. & S. Joiret. 2009. Understanding corrosion of ancient metals for the conservation of cultural heritage. Electrochimica Acta 54 (ELECTROCHEMISTRY DOWN TO THE MOLECULAR LEVEL INTERFACIAL SCIENCE FOR LIFE AND TECHNOLOGY Selection of Papers from the 59th Annual Meetingof the International Society of Electrochemistry7-12 September 2008, Seville, Spain): 5199–5205. DOI: https://doi.org/10.1016/j.electacta.2009.01.036.

Biggs L, Martinon-Torres M, Bellina B, Pryce TO (2013) Prehistoric iron production technologies in the Upper Thai-Malay Peninsula: metallography and slag inclusion analyses of iron artefacts from Khao Sam Kaeo and Phu Khao Thong. Archaeol Anthropol Sci 5:311–329

Bouvet P (2017) Indian Fine Wares. In: Bellina B (ed) Khao Sam Kaeo: a late prehistoric city of the Upper Thai-Malay Peninsula. Ecole française d'Extrême-Orient, Paris

Bray PJ, Pollard AM (2012) A new interpretative approach to the chemistry of copper-alloy objects: source, recycling and technology. Antiquity 86:853–867

Budd P, Gale D, Pollard AM, Thomas RG, Williams PA (1993) Evaluating lead isotope data: further observations. Archaeometry 35:241–246

Bunopas S, Vella P (1992) Geotectonics and Geologic Evolution of Thailand. In: Piancharoen C (ed) National Conference on Geologic Resources of Thailand: Potential for Future Development, 17–24 November 1992. Department of Mineral Resources, Bangkok, pp 209–229

Cadet M, Pryce TO, Dillmann P, Sayavongkhamdy T, Souksavatdy V, Luangkhoth T, Chang N (2022) Technological reconstruction of the late prehistoric primary copper production of the Vilabouly Complex (central Laos). Archaeol Anthropol Sci 14:141. https://doi.org/10.1007/s12520-022-01608-0

Cadet, M., T.O. Pryce, T. Lertchanrit, F. Rispoli, R. Ciarla, P. Venunan & Y. Iizuka (2024) Beyond 'Community Craft specialisation' in prehistoric Mainland Southeast Asian metallurgy: copper smelting behaviours at Khao Sai On, Nil Kham Haeng, Non Pa Wai, Prommatin Tai and Tha Kae in central Thailand. Asian Perspectives 63:189-223. https://doi.org/10.1353/asi.2024.a948117

Cadet M, Tereygeol F, Sayavongkhamdy T, Souksavatdy V, Luangkhoth T, Chang N, Dillmann P, Pryce TO (2021) Late Prehistoric copper smelting in the Lao PDR: Experimental reconstruction

based on the Vilabouly Complex evidence. J Archaeol Sci Rep 37:102932. https://doi.org/10.1016/j.jasrep.2021.102932
Cadet M et al (2019) Laos' central role in Southeast Asian copper exchange networks: A multi-method study of bronzes from the Vilabouly Complex. J Archaeol Sci 109:104988. https://doi.org/10.1016/j.jas.2019.104988
Carter A, O'Reilly D, Shewan L, Dussubieux L (2023) Northwest Cambodia and the Mekong Interaction Sphere: Glass and stone beads from Lovea. Prei Khmeng Sophy 34:77–95
Carter, A.K. 2016. The Production and Exchange of Glass and Stone Beads in Southeast Asia from 500 BCE to the early second millennium CE: An assessment of the work of Peter Francis in light of recent research. Archaeological Research in Asia 6 (Asia's Maritime Bead Trade): 16–29. DOI: https://doi.org/10.1016/j.ara.2016.02.004.
Castillo CC (2017) Archaeobotany Evidence of Exchange Networks and Agricultural Practices. In: Bellina B (ed) Khao Sam Kaeo: An Early Port-City between the Indian Ocean and the South China Sea. Ecole française d'Extrême-orient, Paris https://publications.efeo.fr/en/livres/900_khao-sam-kaeo
Castillo CC, Higham CFW, Miller K, Chang N, Douka K, Higham TFG, Fuller DQ (2018) Social responses to climate change in Iron Age north-east Thailand: new archaeobotanical evidence. Antiquity 92:1274–1291. https://doi.org/10.15184/aqy.2018.198
Changmai P, Pinhasi R, Pietrusewsky M, Stark MT, Ikehara-Quebral RM, Reich D, Flegontov P (2022) Ancient DNA from Protohistoric Period Cambodia indicates that South Asians admixed with local populations as early as 1st–3rd centuries CE. Sci Rep 12:22507. https://doi.org/10.1038/s41598-022-26799-3
Charusiri P, Lunwongsa W, Laochu P (2003) Geophysical Investigations at Khao Nang Klu Lead Deposit, Ban Kli Ti, Kanchanaburi, Western Thailand: Implications for Tectonic Structures Ore Localization and Exploration. Sci Asia 29:265. https://doi.org/10.2306/scienceasia1513-1874.2003.29.265
Cloquet C, Carignan J, Libourel G (2006) Atmospheric pollutant dispersion around an urban area using trace metal concentrations and Pb isotopic compositions in epiphytic lichens. Atmos Environ 40:574–587. https://doi.org/10.1016/j.atmosenv.2005.09.073
Coote, V. 1990. Ancient base metal mines and mining in Southwest Thailand, in I.C. Glover & E. Glover (ed.) Southeast Asian Archaeology 1986, S-561: 131–37 (BAR International Series). Oxford: BAR.
Craddock PT, Meeks ND (1987) Iron in Ancient Copper. Archaeometry 29:187–204
Dussubieux L, Bellina B (2017) Glass from an early Southeast Asian producing and trading centre. In: Bellina B (ed) Khao Sam Kaeo: an early industrial port city between the Indian Ocean and the South China Sea, pp 549–585
Dussubieux L, Bellina B (2018) Glass ornament production and trade polities in the Upper-Thai Peninsula during the Early Iron Age. Archaeol Res Asia:25–36
Dussubieux L, Higham CFW, Pryce TO (2024) Glass circulation in late Iron Age Southeast Asia: New Compositional and Isotopic Data of Beads found at Non Ban Jak in Northeast Thailand. Archaeol Anthropol Sci 16:47. https://doi.org/10.1007/s12520-024-01950-5
Heath H (2020) The ceramic industry. In: Higham CFW, Kijngam A (eds) The Excavation Non Ban Jak, VII. The Fine Arts Department of Thailand, Bangkok, pp 403–432
Higham CFW (2020) The eastern mound: Layers 3 and 4. In: Higham CFW, Kijngam A (eds) The Excavation Non Ban Jak, VII. The Fine Arts Department of Thailand, Bangkok, pp 23–42
Higham CFW, Higham TFG, Petchey F (2020a) Introduction and chronology. In: Higham CFW, Kijngam A (eds) The Excavation Non Ban Jak, VII. The Fine Arts Department of Thailand, Bangkok, pp 1–6
Higham CFW, Kijngam A (eds) (2012) The excavation of Ban Non Wat: The Iron Age. The Fine Arts Department, Bangkok
Higham CFW, Kijngam A (eds) (2020) The Excavation Non Ban Jak., vol VII. The Fine Arts Department of Thailand, Bangkok
Higham CFW, Kijngam A, Talbot S (eds) (2007) The excavation of Noen U-Loke and Non Muang Kao (The Origins of the Civilization of Angkor). Thai Fine Arts Department, Bangkok
Higham CFW, Thosarat R (2004) The excavation of Ban Lum Khao. Vol. 1. 4 (The Origins of the Civilisation of Angkor). Thai Fine Arts Department, Bangkok
Higham TFG et al (2020b) A prehistoric copper-production centre in central Thailand: its dating and wider implications. Antiquity 94:948–965. https://doi.org/10.15184/aqy.2020.120
Hirao Y, Ro J-H (2013) Water Civilisation: From Yangtze to Khmer civilisations. In: Yasuda Y (ed) Chemical composition and lead isotope ratios of bronze artifacts excavated in Cambodia and Thailand. Springer, Tokyo, pp 247–312
Hoppál K, Bellina B, Dussubieux L (2023) Southeast Asia and the Mediterranean World at the Turn of the First Millennium ce: Networks, Commodities and Cultural Reception. Camb Archaeol J:1–24. https://doi.org/10.1017/S0959774323000264
Hutchison CS, Taylor D (1978) Metallogenesis in SE Asia. J Geol Soc 135:407–428
Ingo GM, de Caro T, Riccucci C, Khosroff S (2006) Uncommon corrosion phenomena of archaeological bronze alloys. Appl Phys A 83:581–588. https://doi.org/10.1007/s00339-006-3534-z
Lim TS (2020) Ceramic Variability, Social Complexity and the Political Economy in Iron Age Cambodia and Mainland Southeast Asia (c. 500 BC-AD 500). Australian National University, Canberra https://openresearch-repository.anu.edu.au/handle/1885/205424
Lofile E, Kubiniok J (1996) Landform development and bioturbation on the Khorat plateau, Northeast Thailand. Nat Hist Bull Siam Soc 44:199–216
Manhes G, Allègre CJ, Dupré B, Hamelin B (1980) Lead isotope study of basic-ultrabasic layered complexes: Speculations about the age of the earth and primitive mantle characteristics. Earth Planet Sci Lett 47:370–382
Matsushita T, Matsushita M (2013) Human Skeletal Remains Excavated from Phum Snay. In: Yasuda Y (ed) Water Civilisation: From Yangtze to Khmer civilisations. Springer, Tokyo, pp 181–228
O'Reilly D, Evans D, Shewan L (2017) Airborne LiDAR prospection at Lovea, an Iron Age moated settlement in central Cambodia. Antiquity 91:947–965. https://doi.org/10.15184/aqy.2017.69
O'Reilly D, Shewan L (2015) A report on the 2011-2012 excavation of Lovea: An Iron Age, moated settlement in Cambodia. Archaeol Res Asia 1–2:33–47
O'Reilly D, Shewan L (2016) Phum Lovea: A moated precursor to the pura of Cambodia? Sociopolitical transformation from Iron Age settlements to early state society. J Southeast Asian Stud 3:469–484
O'Reilly D, Shewan L, Domett K, Newton J, Evans D, Vuthy V, Beavan N (2015) The excavation of Phum Sophy 2009-2010: An Iron Age site in North-West Cambodia. J Indo-Pac Archaeol 59:57–73
O'Reilly D, Shewan L, Domett K, Sopheap A (2020) Revisiting Prei Khmeng: The Excavation of an Iron Age Settlement and Cemetery in Cambodia. Asian Perspect 59:33–60
O'Reilly D, von De Driesch A, Voeun V (2006) Archaeology and Archaeozoology of Phum Snay: A Late Prehistoric Cemetery in Northwestern Cambodia. Asian Perspect 45:188–211
O'Reilly D, Scott G (2015) Moated sites of the Iron Age in the Mun River Valley, Thailand: New discoveries using Google Earth. Archaeol Res Asia 3:9–18. https://doi.org/10.1016/j.ara.2015.06.001
Petchey P, Bellina B, Pryce TO, Innanchai J (2018) A late prehistoric iron smithing workshop and associated iron industry at the port

settlement of Khao Sek, Thai-Malay Peninsula. Archaeol Res Asia 13:59–73
Pryce TO (2011) XIX Technical analysis of Bronze Age Ban Non Wat copper-base artefacts. In: Higham CFW, Kijngam A (eds) The excavation of Ban Non Wat: The Bronze Age. The Fine Arts Department, Bangkok, pp 489–498
Pryce TO (2019) Lead Isotope Characterization and Provenance of Copper-Base Artifacts from Ban Chiang and Don Klang. In: White JC, Hamilton EG (eds) Ban Chiang, Northeast Thailand, Volume 2C: The Metal Remains in Regional Context. University of Pennsylvania Press, Philadelphia, P.A., pp 57–64 https://www.upenn.edu/pennpress/book/16044.html
Pryce TO, Bellina B (2018) Bronze bowls and copper drums: Non-ferrous archaeometallurgical evidence for Khao Sek's involvement and role in regional exchange systems. Archaeol Res Asia 13:50–58
Pryce TO, Brauns M, Chang N, Pernicka E, Pollard M, Ramsey C, Rehren T, Souksavatdy V, Sayavongkhamdy T (2011b) Isotopic and technological variation in prehistoric primary Southeast Asian copper production. J Archaeol Sci 38:3309–3322
Pryce, T.O., M. Cadet, T. Lertchanrit, F. Rispoli, R. Ciarla & P. Venunan (2024) Ricardo's Law of Comparative Advantage in Bronze Age, Iron Age and early historic Mainland Southeast Asian metallurgy: copper-base metal production, exchange and consumption behaviours at Khao Sai On, Nil Kham Haeng, Non Pa Wai, Phromatin Tai, Sab Champa and Tha Kae in central Thailand. Asian Perspectives 63:151-188. https://doi.org/10.1353/asi.2024.a948116
Pryce TO, Murillo-Barroso M, Martinon-Torres M, Biggs L, Bellina B (2017a) The Metallurgical Industries, in Khao Sam Kaeo: An Early Port-City between the Indian Ocean and the South China Sea. Ecole française d'Extrême-orient, Paris https://publications.efeo.fr/en/livres/900_khao-sam-kaeo
Pryce TO, Natapintu S (2009) Smelting iron from laterite: Technical possibility or ethnographic aberration? Asian Perspect 48:249–264
Pryce TO, O'Reilly D, Shewan L (2017b) Copper-base metallurgy in Late Iron Age Cambodia: Evidence from Lovea. J Archaeol Sci Rep 13:395–402. https://doi.org/10.1016/j.jasrep.2017.04.005
Pryce TO, Pigott VC (2024) Metal exchange networks in prehistoric Southeast Asia. In: Ludden D (ed) Oxford Research Encyclopedia of Asian History. Oxford University Press, Oxford. https://doi.org/10.1093/acrefore/9780190277727.013.644
Pryce TO, Pigott VC, Martinón-Torres M, Rehren T (2010) Prehistoric Copper Production and Technological Reproduction in the Khao Wong Prachan Valley of Central Thailand. Archaeol Anthropol Sci 2:237–264
Pryce TO, Pollard M, Martinòn-Torres M, Pigott VC, Pernicka E (2011a) Southeast Asia's first isotopically-defined prehistoric copper production system: When did extractive metallurgy begin in the Khao Wong Prachan Valley of central Thailand? Archaeometry 53:146–163
Pryce TO et al (2014) More questions than answers: the Southeast Asian Lead Isotope Project 2009–2012. J Archaeol Sci 42:273–294. https://doi.org/10.1016/j.jas.2013.08.024
Pryce TO et al (2023) A partial prehistory of the southwest silk road: archaeometallurgical networks along the Sub-Himalayan corridor. In: Cambridge Archaeological Journal. Cambridge University Press, pp 1–40. https://doi.org/10.1017/S0959774323000185
Schlosser S, Reinecke A, Schwab R, Pernicka E, Sonetra S, Laychour V (2012) Early Cambodian gold and silver from Prohear: composition, trace elements and gilding. J Archaeol Sci 39:2877–2887
Scott DA (1991) Metallography and Microstructure of Ancient and Historic Metals. The Getty Conservation Institute, Marina del Rey, California
Scott DA (2002) Copper and Bronze in Art: Corrosion, colorants, conservation. The Getty Conservation Institute, Los Angeles https://www.getty.edu/conservation/publications_resources/books/copper_bronze_in_art.html
Selwyn L (2004) Metals and corrosion: a handbook for the conservation professional / by Lyndsie Selwyn. Canadian Conservation Institute, Ottawa
Sitthithaworn E (1990) Metallogenic Map of Thailand. Department of Mineral Resources, Bangkok
Srinivasan S (1999) Lead isotope and trace element analysis in the study of over a hundred South Indian metal icons. Archaeometry 41:91–116
Thirlwall MF (2002) Multicollector ICP-MS analysis of Pb isotopes using a 207Pb - 204Pb double spike demonstrates up to 400 ppm/amu systematic errors in Tl-normalization. Chem Geol 184:255–279
Venunan P (2016) An archaeometallurgical study of iron production in Ban Kruat, lower Northeast Thailand: Technology and social development from the Iron Age (500BC-AD500) to the Imperial Angkorian Khmer (AD802-1431). Doctoral thesis, University College London, London
Venunan P, Ploymukda S, Boripon B, Kwansakul P, Suteerattanapirom K, Pryce TO (2022) A royal wreck? Morpho-technological, elemental and lead isotope analysis of ingots from the Bang Kachai II shipwreck, Thailand. J Archaeol Sci Rep 42:103414. https://doi.org/10.1016/j.jasrep.2022.103414
Venunan P, Pryce TO, Natapintu S, Martinon-Torres M (under review) Resolving resources and reality in early Thai iron markets: Primary production behaviours at Ban Kruat District, Buriram Province, northeast Thailand c. AD 200 - 1450. Archaeological and Anthropological Sciences
White JC, Hamilton EG (2018) Debunking the conventional paradigm: metals and prehistoric society. In: White JC, Hamilton EG (eds) Ban Chiang, Northeast Thailand, Volume 2A: Background to the Study of the Metal Remains. University of Pennsylvania Press, Philadelphia, P.A., pp 49–90
Wilson L, Pollard AM (2001) The Provenance Hypothesis. In: Brothwell DR, Pollard AM (eds) Handbook of Archaeological Sciences. John Wiley & Sons, Ltd., Chichester, UK, pp 507–517
Wohlfarth B, Higham CFW, Yamoah KA, Chabangborn A, Chawchai S, Smittenberg RH (2016) Human adaptation to mid- to late-Holocene climate change in Northeast Thailand. The Holocene 26:1875–1886. https://doi.org/10.1177/0959683616645947
Yankowski A, Kerdsap P, Chang N (2015) Please pass the salt: An ethnoarchaeological study of salt and salt fermented fish production, use and trade in northeast Thailand. Journal of Indo-Pacific Archaeology 37:4–13. https://doi.org/10.7152/jipa.v37i0.14711